Hydrogeology Journal (2021) 29:2561–2594
https://doi.org/10.1007/s10040-021-02339-7

PAPER

Review: Hydrogeology of weathered crystalline/hard-rock aquifers—guidelines for the operational survey and management of their groundwater resources

Patrick Lachassagne[1] · Benoît Dewandel[2,3] · Robert Wyns[4]

Received: 5 July 2020 / Accepted: 19 March 2021 / Published online: 30 April 2021

Abstract

Hard rocks or crystalline rocks (i.e., plutonic and metamorphic rocks) constitute the basement of all continents, and are particularly exposed at the surface in the large shields of Africa, India, North and South America, Australia and Europe. They were, and are still in some cases, exposed to deep weathering processes. The storativity and hydraulic conductivity of hard rocks, and thus their groundwater resources, are controlled by these weathering processes, which created weathering profiles. Hard-rock aquifers then develop mainly within the first 100 m below ground surface, within these weathering profiles. Where partially or noneroded, these weathering profiles comprise: (1) a capacitive but generally low-permeability unconsolidated layer (the saprolite), located immediately above (2) the permeable stratiform fractured layer (SFL). The development of the SFL's fracture network is the consequence of the stress induced by the swelling of some minerals, notably biotite. To a much lesser extent, further weathering, and thus hydraulic conductivity, also develops deeper below the SFL, at the periphery of or within preexisting geological discontinuities (joints, dykes, veins, lithological contacts, etc.). The demonstration and recognition of this conceptual model have enabled understanding of the functioning of such aquifers. Moreover, this conceptual model has facilitated a comprehensive corpus of applied methodologies in hydrogeology and geology, which are described in this review paper such as water-well siting, mapping hydrogeological potentialities from local to country scale, quantitative management, hydrodynamical modeling, protection of hard-rock groundwater resources (even in thermal and mineral aquifers), computing the drainage discharge of tunnels, quarrying, etc.

Keywords Fractured rocks · Crystalline rocks · Saprolite · Stratiform fractured layer · Applied hydrogeology

This article is part of the topical collection "Progress in fractured-rock hydrogeology"

✉ Patrick Lachassagne
patrick.lachassagne@umontpellier.fr

Benoît Dewandel
b.dewandel@brgm.fr

Robert Wyns
r.wyns@free.fr

[1] HSM, Univ Montpellier, CNRS, IRD, Montpellier, France

[2] BRGM, Univ Montpellier, Montpellier, France

[3] G-eau, UMR 183, INRAE, CIRAD, IRD, AgroParisTech, Supagro, BRGM, Montpellier, France

[4] BRGM, Georessources Division, 36009, 45060 Orléans Cedex, BP, France

Introduction

Crystalline rocks, or hard rocks (HR), are plutonic and metamorphic rocks (Michel and Fairbridge 1992); marbles, however, cannot be categorized as HR aquifers as they often constitute karstic aquifers. When unweathered and unfractured, hard rocks such as granites, have low primary porosity and low hydraulic conductivity, whereas metamorphic rocks have lost their original hydrodynamic characteristics through metamorphic processes (Achtziger-Zupancik et al. 2017; Ingebritsen and Gleeson 2017). Although limestones and volcanic rocks (e.g., Charlier et al. 2011 and Lachassagne et al. 2014a for volcanic rocks) can be mechanically hard to drill, as their hydrogeological properties differ, they are not included as HR. Although plutonic granites and metamorphic meta-volcanites, meta-sediments and meta-granites—forming schists, micaschists, quartzites, and gneisses show specific

mineralogy, petrofabrics and textures, they exhibit similar hydrogeological properties and are considered as HR.

Hard rocks form continental basements (Ingebritsen and Gleeson 2017), outcrop over large areas within tectonically stable regions such as ancient cratons, and form over 20% of the earth's surface. Africa contributes about 35% of the world's HR; South and North America about 15% each; India and Australia also have large "HR regions" (Lachassagne et al. 2014b).

The groundwater resources of hard-rock aquifers (HRA) are small in terms of sustainable discharge per productive borehole: from 100 l/h to a few tens of m^3/h (e.g. Courtois et al. 2010; Maurice et al. 2018) as compared to those of porous, karstic and (recent) volcanic aquifers. "Dry" boreholes are also common in HRA (e.g. Courtois et al. 2010). HRA are, however, able to supply water to scattered populations and small-to-medium-size villages, or the suburbs of larger towns. HRA groundwater is often of better quality than surface water and contributes to the well-being of the population and to economic development, especially in arid and semiarid areas where surface-water resources are seasonal and limited to sites adjacent to large rivers. Large parts of Africa, South America, Asia and Australia are reliant on such groundwater resources. In India, HRA water resources greatly contributed to the "Green Revolution" that initially allowed food self-sufficiency in that country (Foster 2012). This has now been partly lost due to aquifer overexploitation and groundwater quality degradation (Maréchal and Ahmed 2003; Dewandel et al. 2007b, 2010; Perrin et al. 2012).

Reviews and research works, particularly by Lachassagne et al. (2014b, 2011) and Dewandel et al. (2006), but also by Worthington et al. (2016), demonstrate that weathering is the main process driving the development of a significant groundwater resource in HR, thus driving the creation of the fractures and then of aquifers in hard rocks.

In fact, if one deals with an historical perspective, this role of the weathering had been described for decades, but mostly for the unconsolidated part of the weathering profile—see for instance Davies et al. (2014) who summarize works from as far back as the 1950s, or Acworth (1987), or Wright (1992). Moreover, as described in the following, several other hypotheses such as tectonics, unloading, etc., were also invoked by hydrogeologists, independently or conjunctly with weathering. These other hypotheses were mainly (and are still in some cases) influencing the methods developed to survey, manage and protect HRA groundwater resources, although not without any drawbacks—see for instance the recent papers from Alle et al. (2017) and Soro et al. (2017). These other hypotheses also constitute (conceptual) limitations that prevent the achievement of results in applied hydrogeology, for instance for the operational modelling of HRA groundwater resources at watershed scale.

Lachassagne et al. (2011) presented a comprehensive review of available papers at the time of its writing, which demonstrates, argument by argument, (1) why the permeable fractures of hard rocks cannot be due to processes other than weathering, and (2) that all the other hypotheses (tectonics and unloading for the most commonly proposed, but several others are listed) either are not grounded on sound demonstrations, or are not demonstrated at all, and are then just hypotheses. This review was completed in 2014 (Lachassagne et al. 2014b).

This paper aims to describe the role of weathering in HRA hydrodynamic properties (hydraulic conductivity, storage) and to present a corpus of efficient operational applications that have been deduced from these genetic concepts. This paper builds upon previous review papers (particularly Lachassagne et al. 2011 and 2014b) with up-to-date research/references that complete and reinforce these results. Most of the references cited in these two previous papers are not cited in this present paper; hence, the interested reader is recommended to consult them as well.

Origin, structure and hydrodynamic properties of hard-rock aquifers

Nonweathered HR have low matrix porosity and low hydraulic conductivity (below 10^{-8} m/s); thus, these rock masses are well-suited for nuclear waste storage (see for instance Figueiredo et al. 2016) at depths greater than several hundreds of metres.

This section describes how HRA include two layers (Fig. 1) forming a composite aquifer (Maréchal et al. 2004; Dewandel et al. 2006, 2011; Lachassagne et al. 2011, 2014b). Their hydraulic conductivity relies on a secondary fracture permeability due to weathering processes (stress induced by the swelling of some minerals, notably biotite). A borehole providing a significant yield of several m^3/h (see section 'Hydrogeological functioning of HR aquifers: hydrochemistry'), crosscuts a decametric (30 to >100 m) layer of low-permeability unweathered rock alternating with a few millimetres to decimetre-thick permeable fractures ("water strikes") created by weathering. Such fractures provide water to the pumped borehole. In granites, subhorizontal fractures appear to be more permeable than the other ones, and notably more permeable than the subvertical ones ($K_{xy} \approx 10\ K_z$; Maréchal et al. 2004).

This transmissive layer, the "stratiform fractured (or fissured) layer" (SFL) forms the aquifer. The unconsolidated superficial zone of the aquifer (the saprolite) is not pervious enough to deliver a significant discharge to common (small diameter) boreholes. However, it is characterised by a significant porosity, enabling leakage towards the underlying fractured layer. This upper layer thus ensures most of the

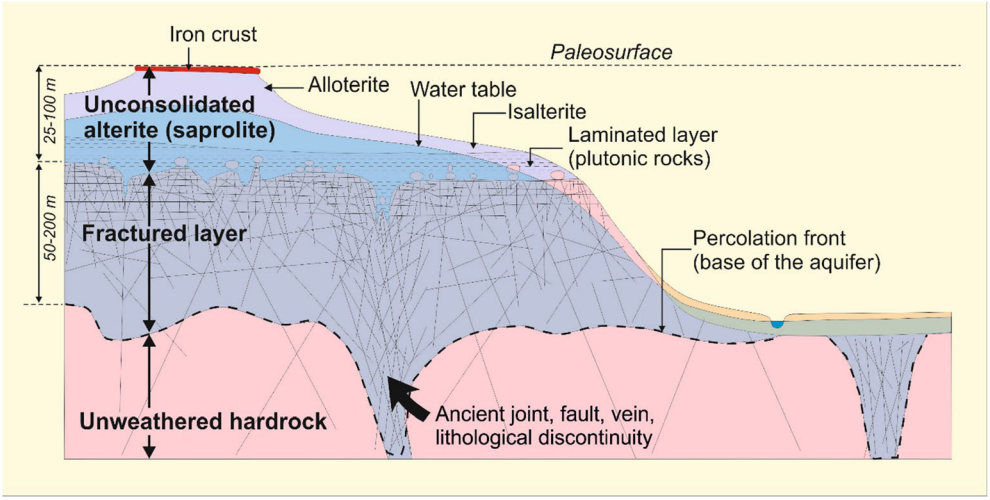

Fig. 1 Conceptual model of a partly eroded paleo-weathering profile on hard rocks (erosion = right part of the figure). Note that all technical terms in this figure are described and explained in section 'Geological structure and hydrodynamic properties of weathering profiles'

capacitive properties of the whole composite aquifer (see also section 'Hydrogeological functioning of HR aquifers: hydrochemistry').

Several hypotheses that are not associated with weathering are still regularly invoked by hydrogeologists to explain the origin of the HRA fractured layer. Lachassagne et al. (2011) and 2014b describe in detail that several authors, in various regions of the world (Africa, India, Australia, Europe, etc.), have acknowledged for several decades the role of weathering in the creation of the unconsolidated part (the saprolite) of the HRA: see for instance Davies et al. (2014), who describe case studies in Africa (Tanzania, Zimbabwe, Nigeria, South-Africa), Madagascar, Asia (Hong-Kong (China), India), and Brazil, and also in Europe, in the UK. However, it is only in the last 15 years that the creation of the fractured layer was demonstrated to be also linked to the same weathering processes (Dewandel et al. 2006, 2011; Lachassagne et al. 2011). This was demonstrated from observations performed by these authors all over the world: France (Dewandel et al. 2017a; Lachassagne et al. 2001c, 2014b; Maréchal et al. 2014; Wyns et al. 2004), South Korea (Cho et al. 2002, 2003), Burkina Faso (Courtois et al. 2010), and India (Dewandel et al. 2006, 2010, 2012, 2017b; Maréchal et al. 2004, 2006), and also from several other observations performed in various regions of France (Brittany, Massif Central, Vosges, Corsica, Pyrénées), other African countries, French Guiana, Madagascar, etc., mostly reported within BRGM reports. The role of weathering in creation of the fractured layer is also directly or indirectly confirmed by the data sets of most of the authors working on HRA. See for instance Davies et al. (2014) and the countries cited previously, as well as Chilton and Smith-Carington (1984), Chilton and Foster (1995), Taylor and Howard (1999, 2000), Chirindja et al. (2017), Dickson et al. (2018), Muchingami et al. (2019) and Vassolo et al. (2019) for Africa; Chambel (2014) for Portugal; Comte et al. (2012) for Ireland; Tan et al. (2017) for Denmark; Riber et al. (2017) for Sweden; Francés et al. (2014) for Spain; Krasny (1996) for Central Europe; Baiocchi et al. (2014, 2016) for the Mediterranean Europe; Chou et al. (2014) and Chuang et al. (2016) for Taiwan; David et al. (2014) for Australia; Riber et al. (2017), Jahns (1943), Hart (2016), Sanford (2017), Meyzonnat et al. (2018) and Setlur et al. (2019) for North America, etc. Even if several authors have not attributed the fractures to weathering processes, some others keep an ambiguity on this genetic relationship, while others do not challenge or discuss this issue at all, at least for the uppermost crust (0–2 km; Achtziger-Zupancic et al. 2017; Ingebritsen and Gleeson 2017).

The main outcome is that the stratiform fractured layer is considered to belong to the weathering profile as well as the above-lying unconsolidated layer (the saprolite; Fig. 1). Worthington et al. (2016) confirm this conceptual model, which is today more and more accepted within the hydrogeological community and used by several authors to explain their observations (see for instance Allé et al. 2017; Baiocchi et al. 2014, 2016; Guihéneuf et al. 2017; Soro et al. 2017; Vouillamoz et al. 2014, 2015; Wubda et al. 2017, etc.).

Previous concepts

Tectonics, unloading processes, and emplacement and cooling of plutonic rocks have been the most common genetic hypotheses formulated to explain the development of fractures within the fractured layer, but without any scientific demonstration of their validity. Lachassagne et al. 2011 and 2014b demonstrated that these hypotheses, briefly summarized in the following, are not relevant to explain the development of HRA.

Jahns (1943) demonstrated that joints in plutonic rocks are unrelated to the emplacement and cooling of these rocks. More annecdotally, Hasenmueller et al. (2017) show that plant roots have no significant impact on HR weathering.

Lachassagne et al. (2011), synthesising previous works in a detailed review paper (see all the references in Lachassagne et al. 2011), demonstrated that:

1. The fractured layer cannot be explained by natural unloading processes. With the exception of some specific conditions such as high cliffs, deep sedimentary basins and artificial unloading (a rapid (hours) decrease of the vertical stress component as in deep wells and mine galleries), there is no existing natural phenomenon able to induce strong compression parallel to the surface. This is the only strain state that may produce subhorizontal fractures such as those commonly observed in granites (described later in this paper). Such an unloading process does not exist in the near subsurface; moreover, such a process would be observed for types of rocks other than HR.
2. Gravity-induced fractures can only be invoked in specific contexts such as high relief such as along the flanks of Alpine valleys, but they do not produce horizontal jointing such as observed in granites.
3. The fractured layer and its associated hydrodynamical properties cannot be explained by tectonic fracturing. Tectonically active areas are mainly at plate boundaries with, nevertheless, to a lesser extent, intraplate tectonics or other processes such as glacial unloading, accommodation in sedimentary basins, etc. Plate boundaries only occupy a few percent of the earth's emerged surface and not thousands to hundred of thousands of km^2 as observed in HR aquifers. The concentration of strain by definition makes them anomalous in regard to the average properties of the crust; therefore, the tectonic fracturing theory faces several inconsistencies. In tectonically stable areas such as most HR areas in the world it requires:

    a. A tectonic process to create the fracture. As explained previously, it is clear that occurrence of such fractures is rare both in time and space. Lachassagne et al. (2011) explain that, with the example of Brittany, France, where the contrast is high between, on one hand, the ~20,000 wells evenly distributed in this region that are delivering HR groundwater, and, on the other hand, the few active tectonic fractures known in this region. Only a few of these wells are located in the vicinity of these fractures. The vast majority of the wells are far away from these active tectonic fractures and statistical analyses do not show any correlation with them.
    b. That the resulting fracture is permeable. It is obvious that a tectonic fracture is a complex structure that is far from being systematically permeable—for instance, Caine et al. (1996) comprehensively describe what a tectonic fracture looks like and show that it comprises several impervious parts. Lachassagne et al. (2011) also summarize several references demonstrating that tectonic fractures act as impervious bodies.
    c. That the resulting tectonic fracture reaches the subsurface, i.e. the depth of a HR borehole, whereas most recent/active tectonic fractures do not reach the last kilometres below ground surface.
    d. That a permeable fracture is not rapidly sealed at the geological timescale, when in fact rejuvenation is overbalanced by fast sealing (in a few years). Outcropping tectonic fractures are often old and thus sealed.
    e. The ubiquity of such fractures. Tectonic fractures are spatially unevenly distributed and thus cannot account for the tens of millions of evenly distributed productive water wells in HR areas of the world (see the example of Brittany already presented).

In addition, further arguments can be put forward: the absence of thermal springs in most of such tectonically stable areas, whereas the main active faults in tectonically active regions quite systematically exhibit several of these thermal springs; and, that most tectonic fractures have a strong dip and should thus hardly ever be tapped by standard boreholes as opposed to the subhorizontal jointing of granitoids and the variously dipping fractures of the other HR fractured layer which are systematically cut by vertical boreholes. Another argument is that lineaments are used to locate "tectonic fractures" but, most of the time, without any demonstration that there is any tectonic fracture at all underlying the identified lineaments and, in some cases, the demonstration that there is no tectonic fracture at all (Soro et al. 2017).

Tröger (U. Tröger, Technische Universität Berlin, personal communication, 2020) raised attention to the fact that Twidale and collaborators "demonstrated" the tectonic origin of the sheet fractures, constituting the fractured layer mostly in granites. As part of this review, several of their papers were studied, and Vidal Romani and Twidale (1999) and Twidale and Bourne (2009) were found to be the most relevant and recent publications on this topic. First, Vidal Romani and Twidale (1999) convincingly show that sheet fractures are due to compressive stress, more precisely horizontal compressive stress. This agrees with the conclusions of, notably, Lachassagne et al. (2011). Second, they show that sheet fractures cannot derive from unloading processes. As exposed previously, this is also one of the conclusions of Lachassagne et al. (2011), independently from the work of Vidal Romani and Twidale (1999), but with several similar proofs and arguments. Third, the remaining issue is to identify the origin of this compressive stress.

Vidal Romani and Twidale (1999) argue that the stress is of tectonic origin, whereas the authors of this review argue

(notably in Lachassagne et al. 2011 and 2014b) that this compressive stress is due to the weathering process at the time it occurred. However, briefly, it is observed that Vidal Romani and Twidale (1999), and also Twidale and Bourne (2009), do not demonstrate convincingly that the compressive stress that creates(ed) the sheet fractures are of tectonic origin. They propose this as a hypothesis (and use often the conditional argument), that, to the authors' opinion, is far from being formally demonstrated. Their argument is mostly to correlate the fact that "many parts of the continents are in substantial compression" (Vidal Romani and Twidale 1999) with the observation of these sheet fractures; however, correlation does not demonstrate causality. They do not consider the other hypothesis of weathering that is much better demonstrated, in the authors' opinion, and can be generalized to all hard rocks, and not only to the sheeting fractures of granites.

Description of the weathering processes that create the stratiform fractured layer (SFL)

The development of the SFL's fracture network is the consequence of the stress induced by the swelling of some minerals. This process was evidenced by Wyns et al. (2003, 2004) and is described in detail by Lachassagne et al. (2014b), who proposed a detailed description and sketches of the deformation ellipsoid, resulting stress and permeability ellipsoid, and the geometry of the induced fracture network as a result of the swelling minerals' orientation configurations: randomly oriented swelling minerals, vertically oriented, horizontally oriented, folded rock. This process is summarized in the following and completed with some additional findings and also references that complete the description of Lachassagne et al. (2014b).

The development of the SFL is thus the consequence of the stress induced by the swelling of some minerals, particularly biotite, olivine and pyroxene, being progressively hydrated and turning into hydro-biotite, then vermiculite, then mixed clay layers, etc. Chemical weathering reactions cause biotite swelling, then volume changes, increasing stress and finally fracturing the rock. In turn, these fractures locally enhance the transport and exportation of chemicals through the rock, accelerating there the weathering. This process of "reaction-induced cracking" is also described by Royne et al. (2008) and was numerically modelled by Rudge et al. (2010) for the carbonation and serpentinisation of peridotite. In all cases (HR, peridotite), the result of the weathering process is then a SFL parallel to the paleotopography contemporaneous with the weathering process (Fig. 1). The numerical model developed by Rudge et al. (2010) was applied by Vasseur and Lachassagne (2019) to granites in order to evaluate the thermal impact of weathering; this last paper also provides additional references on reaction-induced cracking.

The weathering of biotite is an early process. Nevertheless, Anovitz et al. (2021) suggest that it may be preceded by earlier stresses due to crystallization pressures caused by the growing of iron phases that follow pyrite oxidation. The increase in volume of biotite can reach 30% during weathering and that of the total rock 50% (example for a granite). In granular rocks like granites with a quasi-random orientation and location of swelling minerals, the potential expansion tensor is isotropic, but expansion is more difficult in the horizontal plane as the rock extends far away in this direction. Consequently, the horizontal stress component increases during the weathering. In the vertical axis, however, the stress increases until the lithostatic component is offset, then allows vertical expansion, while horizontal stress continues to increase. Consequently, the resulting stress tensor is characterised by a minor vertical component (σ_3), and two major ones (σ_1 and σ_2) that are horizontal (see detailed figures in Lachassagne et al. 2014b). When the stress deviator reaches the elastic limit of the rock, tension cracks appear and the SFL is forming.

Then, for granitic rocks, in accordance with rocks mechanics (Pollard and Aydin 1988; Mandl 2005), the resulting fractures are perpendicular to the minor stress (subvertical) and consequently are subhorizontal, parallel to the gentle topography contemporaneous with the weathering, and lead to the formation of the subhorizontal jointing of granites (Fig. 2). In foliated and folded rocks, the variability of the orientation and location of the minerals able to swell, as well as the ones of the weaker surfaces of the rock (foliation, schistosity), induce fracturing without preferential orientation.

It is the early stage of biotite weathering that induces fracturing. The later stages produce clays which show a tendency to fill newly formed pores of the fractured and weathered minerals. Even if the early weathering of biotites leads to local clogging of biotites and surroundings at a millimeter scale, the density of biotites in the parent rocks is not enough to clog the aperture of all the fractures of the fractured layer at a metre to decametre scale.

Geological structure and hydrodynamic properties of weathering profiles

A typical weathering profile (Fig. 1) comprises layers that have specific hydrodynamic properties. Where and when saturated with groundwater, these layers form a composite aquifer. With depth, the four main layers are (Dewandel et al. 2006; Lachassage et al. 2014b; Vassolo et al. 2019):

1. *An iron or bauxitic crust, that may be absent*. Where preserved from erosion and recharged by heavy rainfall, the iron or bauxitic crust can give rise to small perched aquifers with locally some springs that show an epikarst-


a


b


c


d

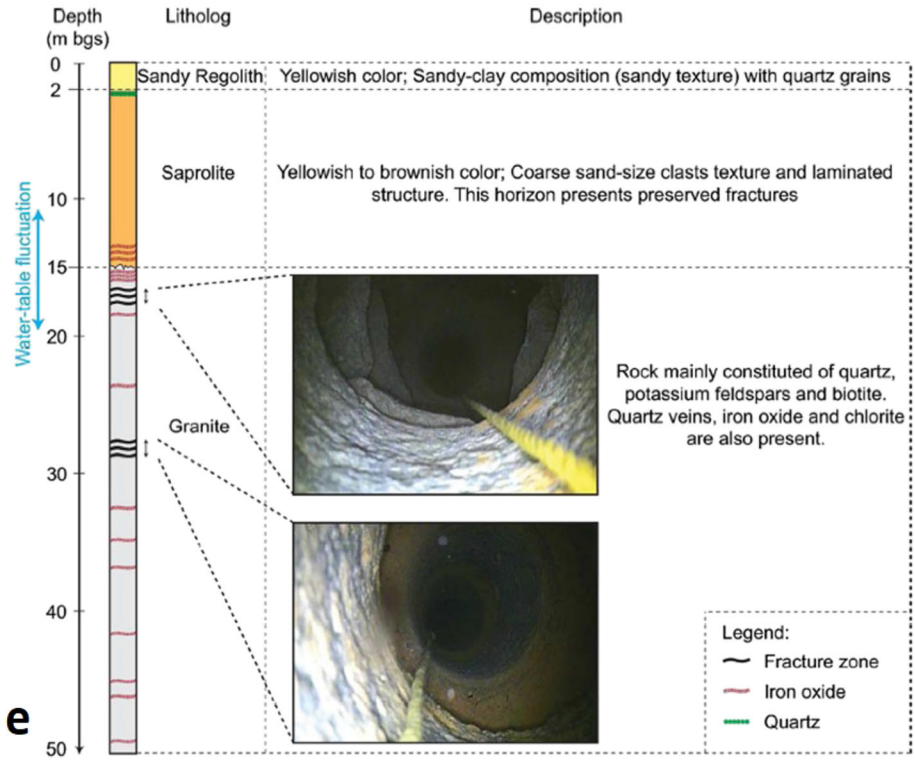
Depth
(m bgs)
Litholog
Description
0
2
10
15
20
30
40
50
Water-table fluctuation
Sandy Regolith
Yellowish color; Sandy-clay composition (sandy texture) with quartz grains
Saprolite
Yellowish to brownish color; Coarse sand-size clasts texture and laminated structure. This horizon presents preserved fractures
Granite
Rock mainly constituted of quartz, potassium feldspars and biotite. Quartz veins, iron oxide and chlorite are also present.
Legend:
Fracture zone
Iron oxide
Quartz
e

◀ **Fig. 2** Various examples of the stratiform fractured layer (the one floor house gives the scale) (SFL): **a** the SFL in the Ploumanach granite, Brittany, France (the total height of the outcrop is about 20 m), **b** the SFL in monzogranite, 14 km SE of Abu Rakh, Saudi Arabia (the hammer gives the scale), **c** upper part of the SFL, Lescastel quarry, Brittany, France, **d** the SFL in biotite-bearing metamorphic volcanic tuffs, Vensat, SW of Gannat, Northern Massif central, France (the height of the photograph is about 2 m), **e** subhorizontal productive fractures in a biotite granite in a 165-mm-diameter unscreened borehole, Choutuppal village, Andhra Pradesh (now Telangana), India. The picture is taken from top to down (**e**), and the yellow rope indicates scale (the well and its exact location are described in Boisson et al. 2015). Photographer R. Wyns (**a**–**d**)

type functioning. These flows are of short duration as the system normally dries up during the dry season; hence, the concentration of iron oxides within this zone aided by evapotranspiration and water throughflow. This is observed in tropical humid regions, as in French Guiana, or during wet season in western Africa.

2. *The saprolite, alterite or proparte regolith*. This is commonly a clay-rich material derived from prolonged in-situ decomposition of bedrock, several tens of metres thick, where this layer has not been eroded. This is commonly a clay-rich material, as most minerals (aluminosilicates) from HR transform into various kinds of clays. However, some rocks such as quartz or microgranite veins, quartzites, etc., mostly composed of silica, do not produce a clay-rich saprolite. In nonplutonics rocks, the saprolite layer is commonly divided into two subunits (Fig. 1): the alloterite and the isalterite.

   The alloterite, at the top of the saprolite, is a clayey horizon where, through volume reduction due to chemical weathering and leaching, the structure of the parent rock is lost. In plutonic rocks, the structure of the parent rock is still identifiable at the top of the weathering profile, which explains that alloterites cannot be identified. In the underlying isalterite, weathering only induces slight or no change in volume thus preserving the rock structure. This layer forms half to two thirds of the thickness of the saprolite layer.

   In plutonic rocks such as granites and gabbros, the base of the saprolite has a laminar form. This "laminated layer" is constituted by the partly consolidated weathered parent rock with coarse-grained clastic texture and a millimeter-scale dense horizontal fracture lamination crosscutting the largest minerals, but preserving the original structure. It was recently demonstrated that the geophysical signature of this laminated layer is shown by an increase in resistivity as compared to both the overlying saprolite and the underlying top of the fractured layer (Belle et al. 2016, 2017), particularly in granites, but also in micaschists.

   The saprolite layer has low hydraulic conductivity. In granite-type rocks, from several studies gathered in Africa and India (Dewandel et al. 2006), the (geometric) mean is 2.10^{-6} m/s for the entire saprolite, with values ranging between 10^{-7} and 5.10^{-6} m/s. The hydraulic conductivity is less in the basal laminated layer (transmissivity about 5.10^{-8}–10^{-7} m^2/s^{-1}; Boisson et al. 2015). The hydraulic conductivity of the alloterite is less than that of the isalterite as the first is more clayey. The hydraulic conductivity is much less in fine-grained rocks' saprolite such as shales, for instance, than in coarse-grained rocks. In these coarse granites, the base of the saprolite can be permeable enough to sustain the discharge of a well, even if it may be difficult to identify if this permeability originates from the base of the saprolite or the top of the SFL.

   Where saturated the saprolite layer ensures the capacitive function of the whole composite aquifer. With its clayey-sandy composition in coarse granites, the saprolite layer has porosities of 5–30% (Compaore et al. 1997). In fine grained or low quartz content schists, the saprolite is clayey with low porosity and hydraulic conductivity.

3. *The SFL* (Figs. 1 and 2), which is characterized by dense fracturing in the first few metres and decreases in density with depth. As described previously, the fractures are mostly subhorizontal in granite-type rocks or in vertically foliated rocks. They are randomly dipping in metamorphic folded rocks (no preferential orientation). In some papers, the top of the SFL, and/or the bottom of the saprolite, where saprolite and boulders coexist, are also referred to as "saprock" (see for instance Wright 1992; Riber et al. 2017).

   The thickness of the SFL is approximately two times that of the saprolite in places where the saprolite was not eroded (Fig. 1) and can reach over 100 m thick (Dewandel et al. 2017a; Wyns 2020a, b). The fracture density decreases with depth towards the base of the weathering profile (the base of the SFL). Then, the observed decrease of the hydraulic conductivity of HRA with depth is not a consequence of a lower permeability of the fractures or of their "closure with depth due to lithostatic constraints", but is rather due to their disappearance in depth (Maréchal et al. 2004; Dewandel et al. 2006).

   Geological logging (or coring) identifies several tens of such fractures in the SFL. Due to healing of some of these fractures, weathering, channeling within fracture plane, etc., only a maximum of four to five fractures are permeable enough to be detected as "water strikes" during borehole drilling and logging, the others being "dry" (see section 'Hydrogeological functioning of HR aquifers: hydrochemistry'). These (max) four to five fractures then ensure the discharge of the well. Sometimes, no fracture at all is permeable enough to ensure a significant discharge. Hence there is a large variability of borehole discharge even for close boreholes; drilling a "dry"

borehole close to a productive one, and vice-versa, is not rare (Maréchal et al. 2004; Dewandel et al. 2006). Then, the SFL of a weathering profile statistically exhibits relatively "homogeneous" properties (thickness, hydrodynamic parameters, etc.), when one considers several wells drilled in this SFL. However, considering the data from each individual well, the standard deviation of the hydrodynamic parameters (notably hydraulic conductivity) is very high, and notably much higher than in most porous aquifers.

Ancient weathering profiles may have been completely sealed as the result of diagenesis due to their burial by marine sediments (Riber et al. 2017; Tan et al. 2017)—for example, in the Vosges Massif (eastern France), the porosity of the SFL of the pre-Triassic weathering profile has been sealed by hydrothermal minerals (ankerite, dolomite, calcite, barite, hematite) during subsidence in the Rhine graben (Wyns 2012); nevertheless, it seems that this sealing can be localized only along faults in old hydrothermal loops (Wyns 2020b). This diagenesis is thought to contribute to the SFL hydraulic-conductivity decrease observed below Cenozoic sediments in another case study in France (Dewandel et al. 2017a).

The properties and hydrodynamic parameters of a granitic SFL in India are described in detail by Maréchal et al. (2004, 2002). The length of each subhorizontal fracture within the SFL is a few tens of metres in diameter (10–30 m). Such a horizontal permeable fracture set is on average 10 times more permeable, and more numerous, than the subvertical joint set. The hydraulic conductivity of these permeable fractures does not show much variability (Maréchal et al. 2004; Dewandel et al. 2006), which supports weathering as a unique origin. The transmissivity of the most conductive part of this 35-m-thick granite SFL reaches 1.10^{-3} m^2/s (Boisson et al. 2015).

The storage coefficient (*S*) in the fracture zone of the same granite aquifer is about 10^{-6} (Boisson et al. 2015). The drainage porosity of this 35-m-thick SFL is 0.5–2% with a partition between blocs and clogged fractures (90%), and permeable fractures (10%) (Maréchal et al. 2004). Dewandel et al. (2010, 2017b) show that the aquifer-scale vertical distribution of the drainage porosity (or specific yield) decreases with depth from 1.5% to 0.2% over a range of depth of 30–40 m below the base of the saprolite.

Dewandel et al. (2012) demonstrate, in a granite aquifer in India (see also Dewandel et al. 2017c for similar results on a peridotite aquifer), the relatively good homogeneity of the SFL hydraulic conductivity at the scale of aquifer subareas. Hydraulic conductivity values range from 10^{-7} to 10^{-4} m/s in the whole aquifer, but are distributed over zones up to 1 km^2 in area with similar hydraulic conductivity. Dewandel et al. (2012) show, at watershed scale, that the effective porosity of the whole aquifer (here a thin saprolite and the SFL) ranges from 0.8 to 2.7% (mean of 1.5%, with an uncertainty below 0.5%). They regionalised and mapped these hydrodynamic parameters over 53 km^2 of aquifer showing that the SFL has homogeneous hydraulic conductivity at few hundred metres to a kilometer scale. These results are useful for modelling groundwater flux and solute transport (sections 'Quantitative management and modeling of HRA groundwater resources at the watershed scale: managed aquifer recharge' and 'Protecting and restoring HRA groundwater resources, groundwater quality modelling, and contaminant transfer'). Dewandel et al. (2017b) report the order of magnitude of the effective porosity at watershed scale, namely 0.3–2%, in two watersheds (700 and 1,000 km^2) in India. Moreover, they show that the vertical distribution of effective porosity can be very different from one place to another at the scale of the same aquifer, and that the fractured layer is not always characterized by a rapid decrease of the effective porosity with depth. Locally, lateral variations in effective porosity can be larger than vertical ones.

The SFL assumes the transmissive function of the composite aquifer. It is drawn from most of the boreholes drilled in hard-rock areas. In some regions, due to erosion, the covering saprolite layer may have been partially or totally eroded; it may also be unsaturated due to low piezometric levels. In these cases, the SFL assumes not only the transmissive function of the aquifer, but also its capacitive one, which is for instance the case in Brittany (France), where, due to the erosion of the saprolite, 80–90% of the stored groundwater is found in the fractured layer (Wyns et al. 2004).

4. *The fresh basement* This is only permeable where "deep fractures" are present (see section '"Deep vertical" discontinuities in the unweathered basement'). Even if these fractures are as permeable as the fractures of the SFL, their density with depth and laterally is lower (Cho et al. 2003). Then, for catchment-scale water resources studies, the fresh basement is considered as impermeable with a negligible storativity (Maréchal et al. 2004)

Main parameters governing HRA development (weathering profile development) and their structure

The development of a weathering profile, and thus of HRA, requires several criteria:

- The HR must be located *above sea level* and not covered by a thickness of sediments.
- Development of a weathering profile tens of metres thick must have enough *time* for effective hydrogeological development; this takes millions to tens of millions of years (Myr) to create (Wyns 2002; Wyns et al. 2003). If there is

no erosion (see the following), the regolith thickness increases as the square root of time (Braun et al. 2016).

- As weathering requires *water*, hot or cold deserts are not favorable for weathering, nor areas of permafrost (Acworth 1987; Wyns et al. 2003). However, due to continental drift, climatic changes at the geological time scale, and duration of a weathering profile functioning, many cases of weathering profiles are observed in present desert countries (e.g. Saudi Arabia, Fig. 2b).
- There must be *stable geodynamic conditions*. The erosion rate must be lower than the weathering rate (Wyns et al. 2003; Braun et al. 2016), allowing the weathering profile to grow and to thicken leading to peneplaination. Due to erosion, tectonically active processes do not favor weathering profile conservation. In fact, weathering profiles of lateritic type are characterized by the leached removal of dissolved compounds from the rock. Profiles submitted to a gentle regional uplift (such as long-term lithospheric deformation) favor the development of thick weathering profiles, with a SFL over 200 m thick (Wyns 2020a; Cho et al. 2002; Monod et al. 2016).
- *Temperature*, linked to the climate, is a secondary factor that only affects the kinetics of the weathering process, with a factor of 1.7 between a tropical (28 °C) and a temperate climate (15 °C; Oliva et al. 2003). Moreover, the characteristic period of the climate stability, 10^4 to 10^5 years, cannot explain the time required to develop the weathering profiles which is much longer (10^7–10^8 years; Wyns et al. 2002). The characteristic period is thus mostly of geodynamic origin (Wyns 2020a). In addition, the present climatic belts are not older than 10 Myr, due to the late Miocene to Quaternary formation of polar ice caps: palynology and stable isotope data show that lateritic weathering was possible up to 60° of latitude. Most of the iron or bauxitic surfaces in modern tropical countries are then also related to ancient weathering profiles (Theveniaut and Freyssinet 1999 and 2002).

Differential weathering results in a local topographic scarp separating less weatherable rocks from lower more weatherable ones; this "scarp" is also present at depth at the interface between the various layers of the weathering profile. Leucogranites, quartz and microgranite veins and pegmatites, generally weather less than the surrounding biotite granite (Hill 1996; Lachassagne et al. 2001c; Dewandel et al. 2006, 2011). Within metamorphic lithologies, harder quartzite layers and green rock intrusions stand proud of surrounding schistose rocks in the weathering profile. Within calc-silicate gneisses, harder granite veins weather less and stand proud of the surrounding strata (Maréchal et al. 2014).

To summarise, mineralogy and texture are the main controls of differential weathering, biotite-rich and coarse rocks being the more weatherable; however, at watershed scale, a case-by-case geological study is needed to show the effects of differential weathering. As the geodynamical context changes (i.e., when passing from no tectonic activity (peneplaination) to active tectonism) the weathering profile is partially or totally eroded. Conditions again favorable for the development of a new weathering profile favour the development of a polyphased weathering profile (Dewandel et al. 2006; Lachassagne et al. 2014c); thus, most HR areas of the world show relicts of several generations of weathering profiles (Jahns 1943; Chilton and Smith-Carington 1984; Theveniaut and Freyssinet 1999, 2002; Thiry et al. 2005; Dewandel et al. 2006).

In Europe, periods of weathering profile formation have been recognised from the Carboniferous, Permian, Triassic and Liassic. The Early Cretaceous and the Early and Middle Eocene, having lasted 45 and 25 Myr, respectively, are the most recent period during which weathering processes lasted long enough to develop 70–100-m-thick profiles that included a 50–70-m-thick fractured layer underlying a 20–30 m layer of saprolite (Wyns et al. 2003; Bauer et al. 2016). The late Miocene to Present period only produced thin profiles that have little hydrogeological significance (Lachassagne et al. 2014c).

Complex weathering profiles result from multiphase periods of weathering and erosion (Taylor and Howard 1999, 2000; Dewandel et al. 2006), and, in some cases, resedimentation as "pediment formations" (Chardon et al. 2018). For instance, recent weathering periods produced a 5–8 m thick (below the current topographic surface) weathering profile in South Korea (Cho et al. 2002; Fig. 3) and a 2–3-m thick weathering profile in France (Lachassagne et al. 2014c). This recent weathering clearly developed after the main earlier weathering phase(s): Late Cretaceous to early Eocene period in France, with hard rock weathering profiles about 80 m deep, including a thick hydraulically effective SFL. In fact, this recent weathering crosscuts all the horizons of the ancient Late Cretaceous to early Eocene weathering profile. This recent phase follows the present topographic surface. Since these recent weathering phases have not developed a thick fractured layer, they are of low hydrogeological interest, but must be considered as they can mislead weathering profile mapping (section 'Assessing HRA groundwater reserves from watershed to regional scales').

In the Cacao village area, French Guiana (Fig. 4; Courtois et al. 2003), a polyphased weathering, uplift and erosion history formed the complex weathering profile, with four stepped palaeo-erosion surfaces including the present-day fluviatile topography. This case study comprises juxtaposed amphibolite metamorphic rocks and a granodiorite; hence, differential weathering is also observed between these rocks—the amphibolite metamorphic

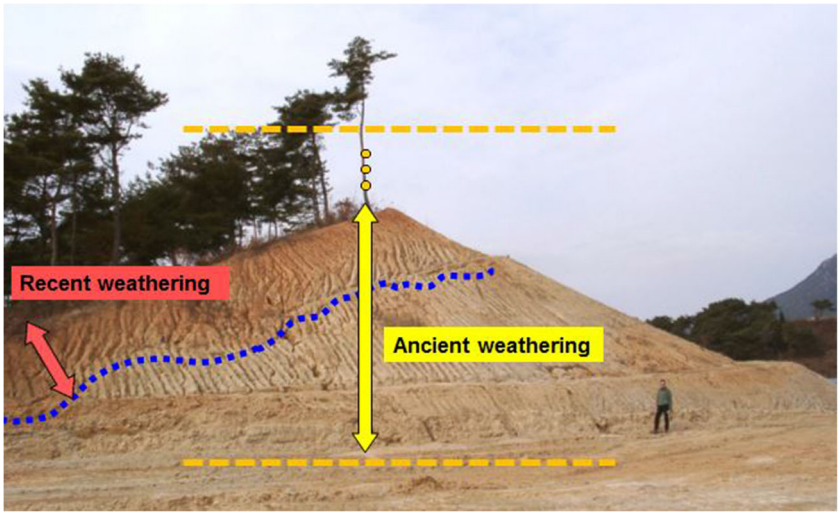

Fig. 3 Red recent weathering, related to the present-day topography, intersecting a much older weathering profile, Namwon area, South Korea. Photographer P. Lachassagne

rocks weather less and stand "in relief" compared to the granodiorite.

Consequently, and as a conclusion, weathering profiles are not the result of present-day climate but of ancient ones. That is why Norway and Scotland (UK), as well as France, Central Europe, the Korean Peninsula, North America, etc., exhibit such weathering profiles. Globally, individual regions exhibit characteristic weathering profiles indicative of the paleo- (and present day in some cases) tectonic context (and erosion processes) they have experienced. The main determinants of such weathering profiles are not the climate, but geodynamical factors such as morphology, erosion rate, duration of tectonic stability, and the presence of water. Present-day arid or semiarid regions as well as permafrost zones may exhibit relicts of ancient weathering profiles, like in the Arabian and Scandinavian shields or in Greenland (Wyns 2020a).

In some areas of significant relief, ancient weathering profiles may be partly or totally eroded, but they may have been preserved by a sedimentary rock cover and latterly revealed by erosion. In the latter, an ancient weathering profile, like pre-Triassic or Early Cretaceous profiles of the Hercynian French Massif Central and Armorican Massif, can be reactivated. The late Tertiary and Quaternary weathering profiles formed on fresh rocks are less developed with a small thickness 5–30 m (Lachassagne et al. 2014c).

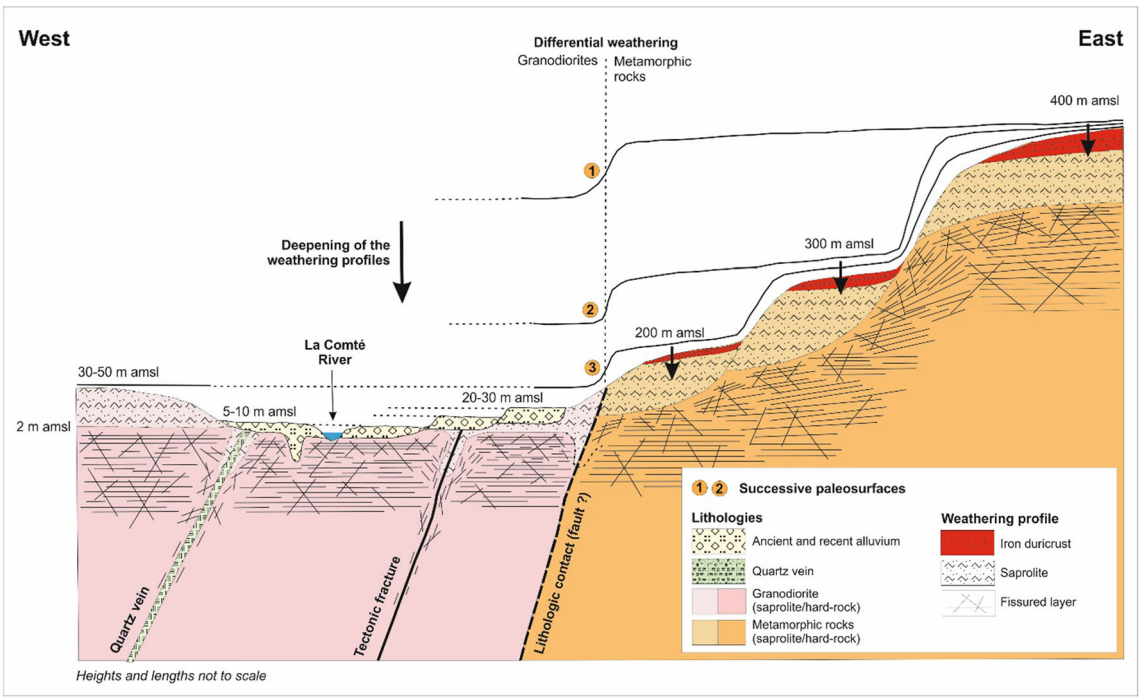

Fig. 4 Differential and multiphase uplift, erosion and weathering in the Cacao village area, French Guiana, from Courtois et al. (2003)

Ferric oxide caps mainly occur in present-day tropical countries with a long dry season. However, relict weathering profiles are locally present in France (Thiry et al. 2005). The absence of iron duricrust at the top of lateritic profiles is due either to erosion of the profile surface before burial by sediments, or to rehydratation of the hematitic duricrust to iron hydroxides (goethite and limonite) within a latosol. This absence is not due to the present-day temperate climate.

Mapping the layers (saprolite, SFL) constituting the hard rock aquifers

This conceptual model shows how HRA can be considered as "continuous aquifers" being formed of superimposed layers, even though hydraulic conductivity heterogeneities exist between each layer and in the SFL. Therefore, it is possible to map, or model in three dimensions, the elevation and thickness of HRA constituent layers (Lachassagne et al. 2001c; Wyns et al. 2004; Dewandel et al. 2006). The saprolite layer has mostly capacitive hydrodynamic properties, while the SFL has transmissive properties and some capacitive properties.

This mapping methodology is based on topographic maps, digital elevation models (DEM), field (outcrops, dug wells) geological observations, borehole data, field geophysical surveys (see Allé et al. (2017); Belle et al. (2017); Soro et al. (2017); Wubda et al. (2017) for a good overview of the application of electrical geophysical methods to HRA), aerial geophysical surveys (Chandra et al. 2016), and hydrodynamical data (Fig. 5). It is a two-fold methodology:

– First, within a study area, characterise the local weathering history (eventually multiphase), and also the weathering profiles for the main rock types, to explain any differential weathering (Fig. 4). Identifying also "paleosurfaces" (see section 'Main parameters governing HRA development (weathering profile development) and their structure').
– Second, map the elevation of the interfaces separating the saprolite base at the SFL top and the SFL base (top of the unweathered basement). These interfaces are generally parallel to the paleosurfaces.

The methodology varies according to data availability and the presence of outcrops. The resulting maps (Fig. 6) show the intersection of these horizons with topography similarly in a geological map (Fig. 6a), isohypses of these interfaces (Fig. 6b), and map of layer thickness variation (Fig. 6c). Such a mapping methodology can be implemented at various scales, from local (Figs. 4 and 6) to country scale (e.g. Courtois et al. 2010), or even continental scale (Wilford et al. 2016).

The geometry of the saprolite base is determined using borehole data, geophysical data and geological field surveys. Where the saprolite basal surface is cut by the present-day ground surface, as by valleys, it is possible, in the field, to determine from outcrops the position of the saprolite/weathered-fractured layer interface. Using observations/computations of the SFL thickness from outcrop and analysis of borehole data (Courtois et al. 2010), the SFL base elevation is calculated by substracting SFL thickness from the elevation of the base of the saprolite.

The elevations of (1) the saprolite/SFL interface and (2) the SFL/fresh rock interface can be subtracted from ground surface from DEM data, to calculate the residual thickness of the saprolite and SFL. In regions where the

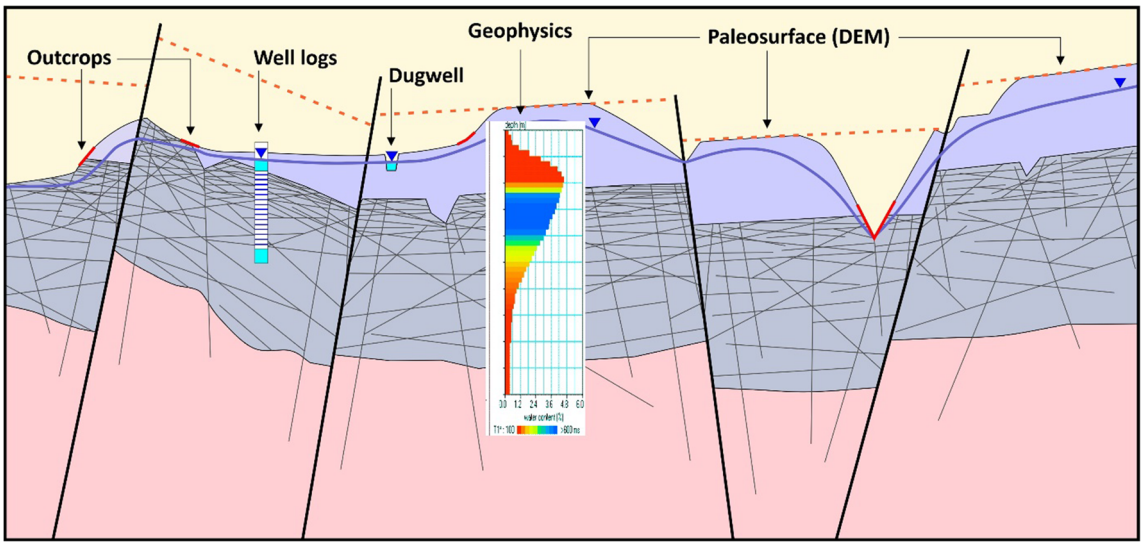

Fig. 5 Methodology and data used for mapping HRA layers. See also the geological legend in Fig. 1. Note that the vertical scale is exaggerated, but that the relative thicknesses of the saprolite and SFL (1/3–2/3) are correct

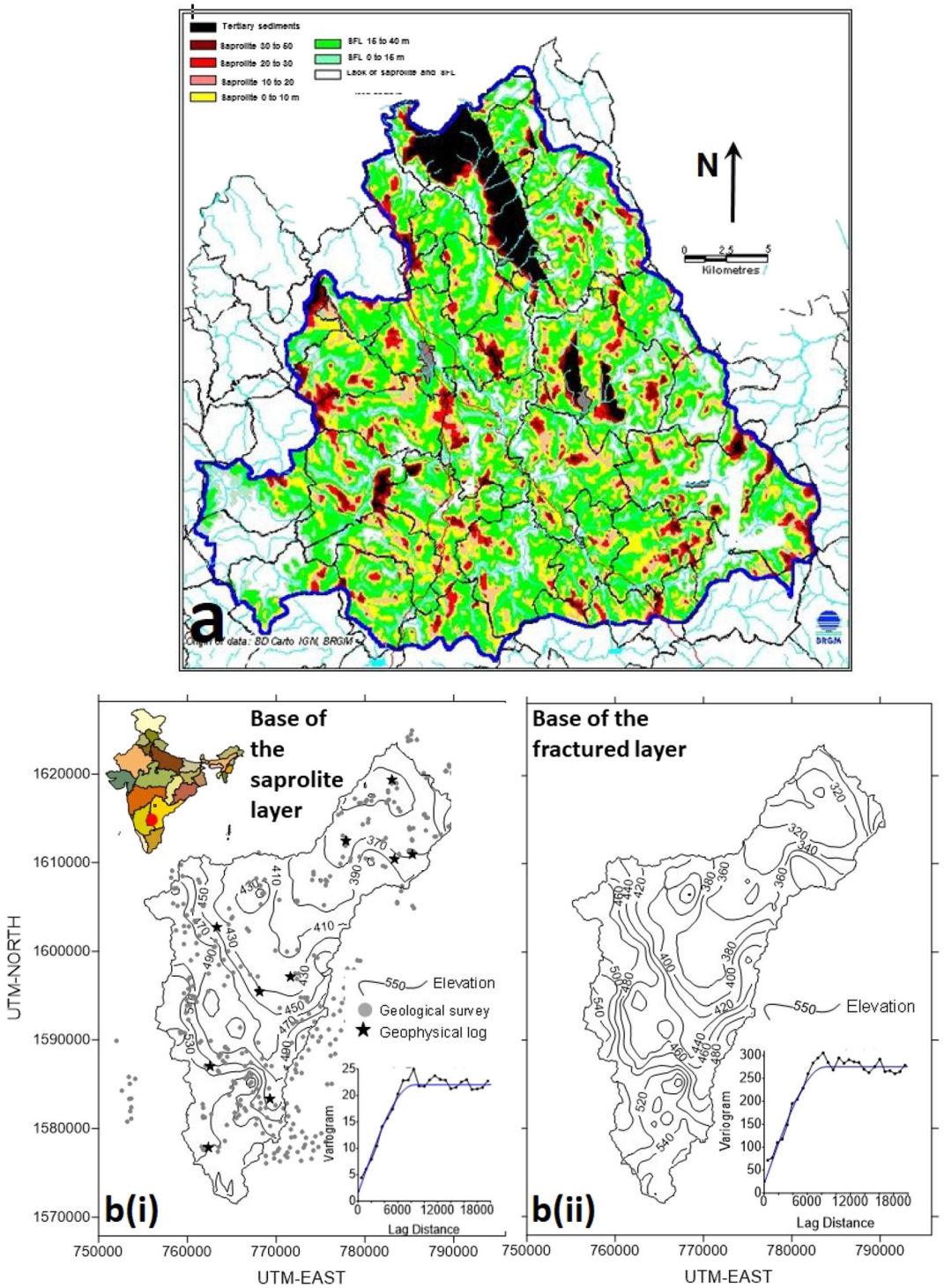

Fig. 6 Examples of maps of the various layers forming hard-rock aquifers: **a** geological map of the weathering cover on the Truyère River, Lozère, France, watershed (700 km^2): thickness of saprolite (increasing thickness from yellow, 0–10 m, to red and black, >50 m) and the fractured layer (increasing thickness from blue, 0–15 m, to green, 15–40 m), white: weathering profile totally eroded (Lachassagne et al. 2001c) with permission from Wiley; **b** ~730-km^2 isohypse map of the elevation (in m above sea level) of (**bi**) the base of the laminated layer (base of the saprolite) and (**bii**) of the base of the SFL (= top of fresh and unfractured basement), Anantapur, Andhra Pradesh (now Telangana), India (from Dewandel et al. 2017b). With permission from Wiley

paleosurface(s) are partly preserved from erosion, slope analysis from DEM data can be used to reconstruct paleosurfaces confirmed by field observations (outcrops, drillings). This mapping methodology can be applied at local (a few hectares to square kilometres) to regional (a whole country) scales.

Observation of weathering at HR outcrops requires differentiation of limited "recent weathering" (e.g. Fig. 3) from thicker weathering profiles; recent weathering is usually only a few metres deep (see for instance the nice picture of such a recent saprolite developed on an older eroded weathering profile, in Fig. A1a of Setlur et al. 2019). Limited "recent weathering" indicates that the associated SFL will not be hydrogeologically significant (section 'Main parameters governing HRA development (weathering profile development) and their structure'). Recent weathering can transform a near-surface weathering profile (SFL, fresh rock) into a thin few metres of saprolite where the previous layers cannot be yet distinguished. Thus, observation on shallow outcrops must be completed with deeper ones, for instance in quarries or in deep trenches, as well as with borehole or geophysical data, to distinguish shallow recent weathering (not significant hydrogeologically) from the older (significant) weathering profile; thus, characterizing the local weathering history is all important.

Observations on outcrops also enable the identification of the SFL (see for instance Fig. 2) and, more precisely the location of the observed outcrop within the SFL (top, medium, bottom) according to the density of the fractures. Electrical geophysical methods, e.g. electrical resistivity tomography (ERT) are particularly well suited for identifying and mapping the various layers constituting weathering profiles. Definitely, as weathering profiles are three-dimensional (3D) objects, at least two-dimensional (2D) methods such as ERT, must be employed. Alle et al. (2017) nicely show the important artifacts due to the implementation of one-dimensional (1D) methods; they show that a near-surface clayey anomaly (a patch) within the saprolite can be interpreted similarly as a deep subvertical conductive structure. Moreover, they also show that deep subvertical conductive structures such as those searched for by some hydrogeologists, can not at all be detected from the surface with 1D profiling or vertical electrical soundings.

Belle et al. (2016, 2017) identify the specific electrical signature of the laminated layer in granites, and even in micaschists. It appears on most profiles as a more resistant layer than the overlying saprolite and the underlying SFL, which must not be mistaken for unweathered boulders (corestones) remaining within the bottom of the saprolite. The identification and location of this laminated layer is needed to measure the remaining thickness of the saprolite, thus its groundwater storage capacity, and also to locate the underlying SFL, which is of interest for water-well siting.

From a methodological standpoint, Belle et al. (2017) also show the influence of the chosen ERT inversion method. A given ERT inversion method can highlight or, on the opposite, partially or totally hide some geological structures. Some inversion methods provide evidence of subvertical structures (e.g., standard vertical), whereas some other methods provide evidence of subhorizontal structures (e.g., standard horizontal) such as can be found in the various layers of the weathering profile. In the Belle et al. (2017) case study, the resistive laminated layer is nevertheless found by all inversion modes, even where the layer thickness and extent are small.

"Deep vertical" discontinuities in the unweathered basement

Authors such as Chilton and Smith-Carington (1984); Acworth (1987); Sander (1997); Owen et al. (2007); Dewandel et al. (2011) and Place et al. (2015), describe preexisting heterogeneities within the HR—such as quartz, pegmatite and aplite veins; dolerite dykes, ancient faults and joints; and contacts between lithological units (Neves and Morales 2007; Le Borgne et al. 2004, 2006; Durand et al. 2006; Roques et al. 2016), that act as sites for preferential weathering. At such sites, local deepenings of the weathering profile are reported to reach several hundreds of metres below ground surface (Roques et al. 2014b). The weathering process is at the origin of fracture development and enhanced local hydraulic conductivity in the HR surrounding these heterogeneities. The weathering process is also at the origin of the fracturation within meter- to decameter-wide discontinuities such as quartz veins and pegmatite veins (Dewandel et al. 2011; Figs. 1 and 7). This deep weathering can locally enhance hydraulic continuity between the subsurface (HR or alluvial) aquifers and these deep structures (Roques et al. 2014b) and special attention has to be paid for evaluating their hydrodynamic properties, their relationships with the surroundings weathered layers, and consequently their sustainable yield (Dewandel et al. 2014).

Near these discontinuities, the HR weathering-profile saprolite and SFL are characterised by a deepening of weathered layers in the HR close to the contact. There the stress tensor is deviated and σ_3 becomes suborthogonal to the heterogeneity; consequently, the fractured layer is "verticalised" as it develops parallel to the vein or the former fault/joint/contact (Fig. 7). There, the fractured layer and saprolite reach greater depths—by up to several hundred metres (Dewandel et al. 2011; Roques et al. 2014b; Arias et al. 2016; Belle et al. 2017)—than within the classic subhorizontal previously described profile. However, these layers are not wide on the sides of the discontinuity. Such geological structures are of primary hydrogeological interest in areas where the SFL has been eroded or is unsaturated above the piezometric level. In these areas, they form the only targets for water-supply boreholes.

Dolerite dykes also form weathering products, however with properties that define them as having low hydrodynamic potential. Such discontinuities, not enhancing the thickness or hydraulic conductivity of the weathered saprolite or SFL in granite, nor its hydraulic conductivity, make poor hydrogeological targets (Dewandel et al. 2011; Perrin et al. 2011a). They can

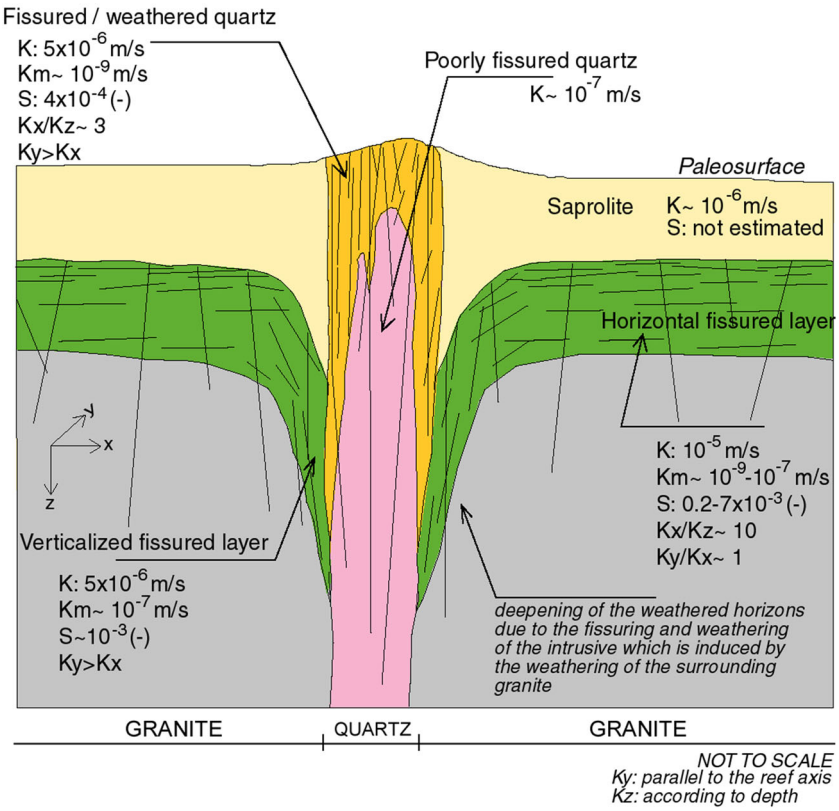

Fig. 7 Conceptual hydrodynamic model of a vertical discontinuity in hard rocks (Dewandel et al. 2011). The parameters for the SFL are from Dewandel et al. (2006), cited in (Dewandel et al. 2011); both papers provide ranges and variances. Km means matrix hydraulic conductivity. With permission from Elsevier

even act as impermeable boundaries to groundwater flow, and, as such, have an impact on the piezometry.

Some of the low-permeability structures are large, e.g. up to 500 m in a granite case study near the border of an Oligocene graben in the Massif Central in France (Belle et al. 2016 and 2017, Dewandel et al. 2017a). There, the saprolite depth reaches more than 200 m (the depth of the deepest borehole, that did not reach the bottom of the saprolite). The two boreholes sited in these structures are of low productivity: only 0.5 m^3/h for each of these 150-m deep boreholes totally screened in this saprolite-type formation. Similar deep weathered structures, to 250 m depth, are described along the contact between the metamorphic rock and an underlying granite (Arias et al. 2016). Such large structures need to be represented in the weathering-profile geological-mapping process as they must be avoided for siting water boreholes but included in groundwater reserve evaluation and groundwater modelling.

Hydrogeological functioning of HR aquifers: hydrochemistry

The HRA are characterized by a rather low hydraulic conductivity, showing then high hydraulic gradients (often over 1%), notably in the parts of the world where the recharge is significant. Consequently, piezometric heads are there subparallel to the topographic surface (Figs. 8 and

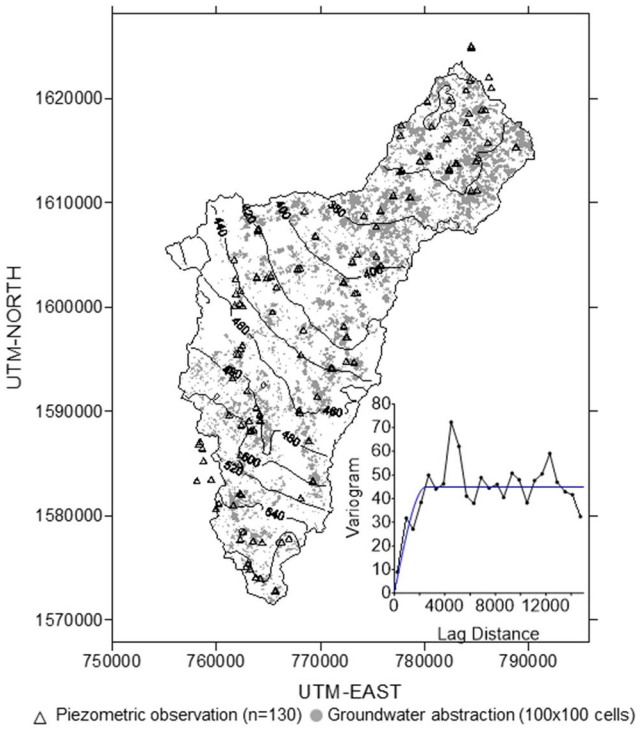

Fig. 8 Piezometric map (in meters above sea level) on the 730-km^2 Anantapur watershed, Andhra Pradesh (now Telangana), India, and groundwater abstraction (on 100 m × 100 m cells; in grey); from Dewandel et al. (2017b). With permission from Wiley

9a). Under natural conditions, piezometric contours beneath watersheds are often similar to the surface topography. Groundwater watersheds are very similar to surface-water watersheds (Fig. 9).

Except in areas of low recharge and over-exploited areas, piezometric levels are shallow (Fig. 9a). Streams drain aquifers in wet temperate and tropical humid regions where streams flow during the wet season, and topographic depressions include "spring zones" (and/or wetland areas) with groundwater issuing from HRA. Due to the low hydraulic conductivity of these composite aquifers, rivers' specific discharges are low in HR areas, below 2 L/s/km^2 (Baiocchi et al.

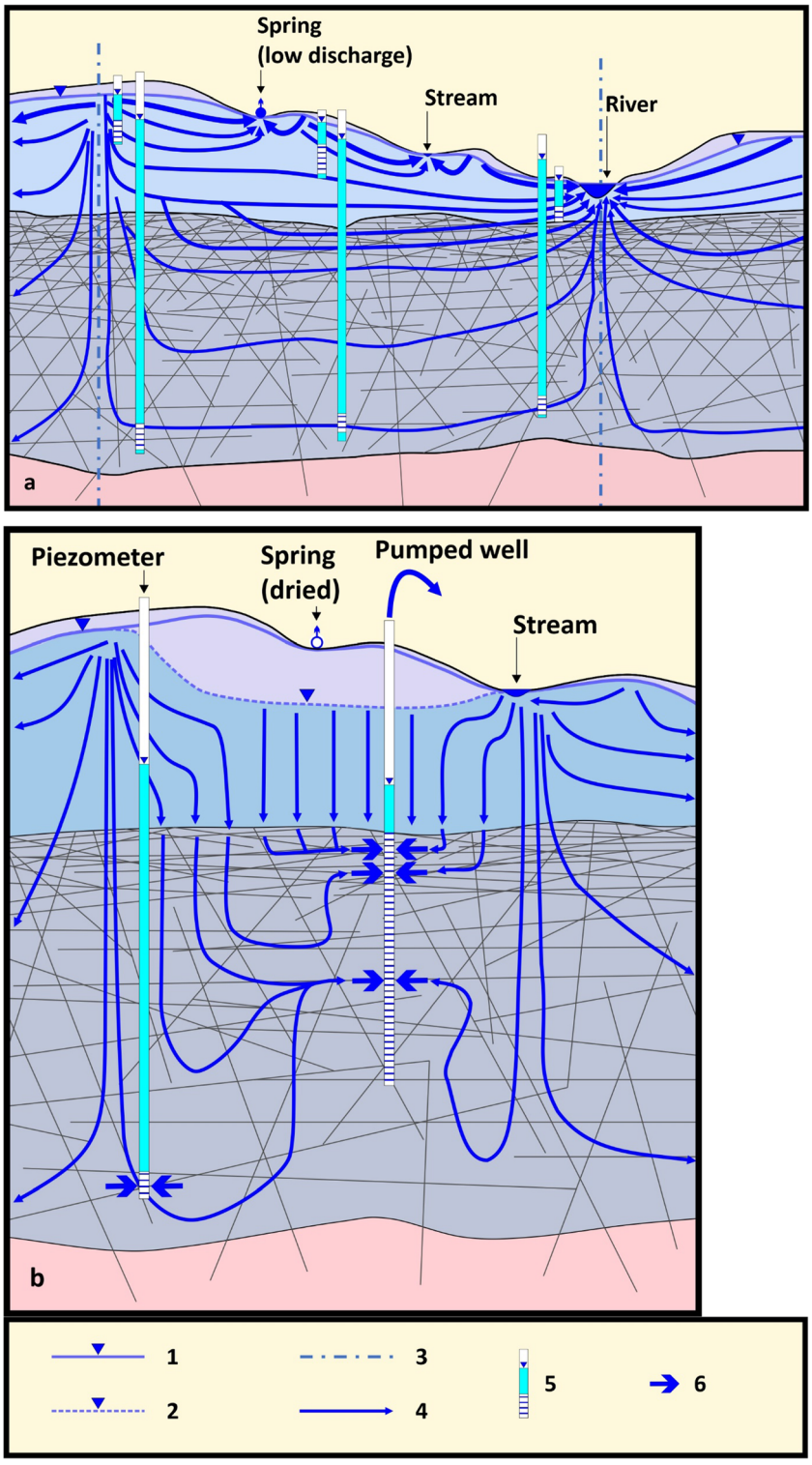

Fig. 9 Hydrogeological functioning of hard-rock aquifers **a** in natural flow conditions and **b** in pumping-induced conditions (borewell pumped in the SFL). The geological legend is the same as those of Figs. 1 and 5. The two main layers (saprolite and SFL) are clearly delimited, as well as the unsaturated zone, and the hydraulic heads in each layer are described (water table, piezometers). Legend: 1. Piezometric level (water table) in the saprolite (**a**–**b**) and also without any pumping or before pumping (**b**); 2. piezometric level (water table, **b**) in the saprolite after the well was put in operation and pumped for a while. Quadratic head losses in the borewell are not shown; 3. Hydrogeological water divide; 4. Groundwater flow lines (**a**, the thickness of the flow lines is proportional to the groundwater flow); 5. Borewell/piezometer with, from bottom to top: screened interval, tube filled with groundwater, and piezometric level (triangle). The tube is grouted; 6. Location of the main water strikes in the borewell/piezometers (**b**)

2016; Dewandel et al. 2004). Consequently, most springs have also a low discharge.

In areas where the piezometric level reaches the topographic surface, springs and rivers drain the aquifer, and groundwater/surface-water interactions occur. This is the aquifer's "discharge area". This "discharge area" cannot be opposed to an upstream "recharge area" of the aquifer. In fact, as the aquifer is unconfined, the whole aquifer watershed contributes to its recharge (Fig. 9a).

Both direct (diffuse) and indirect (localized) recharge, as defined by Lerner (cited by Marechal et al. 2006), are documented in hard-rock aquifers. Maréchal et al. (2006) quantify both direct and indirect recharge at the aquifer scale. In regions with a relatively high recharge amount—like in the Sudanian subsahelian zone in Africa (Wubda et al. 2017, Babaye et al. 2019) or in Ireland (Cai and Ofterdinger 2016)—direct recharge occurs either through the saprolite (or the SFL if it outcrops) and/or reworked superficial formations (Cai and Ofterdinger 2016). In regions with a low recharge amount (like in the Sahelian zone in Africa), indirect recharge prevails. The recharge occurs more in the lower parts of the watershed, in the flats or "bas-fonds", for two main reasons:

1. The highest parts of some watersheds can have thicker remains of low-hydraulic-conductivity clayey alloterites (or even duricrust) that inhibit infiltration and allow runoff that accumulates in the flats as seasonal ponds.
2. In arid environments, aquifer recharge is low. Effective recharge to aquifers occurs in valley bottoms where runoff accumulates into temporary ponds during the major rainfall events (Leblanc et al. 2008). Elsewhere in the watershed, direct recharge is very low to nil. Wubda et al. (2017), in Burkina Faso and Benin, show that the infiltration does not take place at the center of the pond to the aquifer, but occurs laterally in its banks.

Under "natural" conditions, most groundwater flow results from recharge in the upper aquifer layer (saprolite). Then the water flows to ephemeral or perennial streams or spring, through the saprolite (Fig. 9a). Due to compartmentation of the SFL, its "regional" hydraulic conductivity is poor; only a small proportion of the recharge reaches the deepest fractures (Alazard et al. 2016). Therefore, aquifer groundwater age increases with depth (Armandine Les Landes et al. 2015; Roques et al. 2014a), and mineral content increases by water–rock interactions, and with the part of the weathering profile in which the groundwater is flowing (e.g. Chabaux et al. 2017; Babaye et al. 2019). Consequently, the composite aquifer may show a strong vertical hydrogeochemical stratification, both in the saprolite (Durand et al. 2006; de Montety et al. 2018) and in the SFL (Alazard et al. 2016)—for example, in some watersheds, there is an increase of fluoride concentration with depth (Pauwels et al. 2015), and an increase of ages with depth, even in the saprolite (de Montety et al. 2018). In Brittany (France), de Montety et al. 2018 in fact showed that the groundwater mean residence time at the bottom of a 15–20-m-thick saprolite layer can reach 10–15 years.

Where the saprolite is thin (due to its erosion), as on the granites of central India (Alazard et al. 2016), the aquifer recharge process comprises several stages with (1) mostly vertical diffuse piston flow in the saprolite as well as preferential recharge fluxes through preserved fractures in the saprolite and, below, (2) preferential deep horizontal flow in the SFL. Direct vertical percolation is limited to the recharge period (monsoon); then newly recharged water mixes with groundwater in the aquifer both vertically and horizontally. Different "water bodies" of varied hydrochemistry can then be distinguished within the aquifer, evolving according to the hydrological conditions and recharge structures. In wet regions where the saprolite has been removed, for example due to glacial erosion, the stratiform fractured layer is often very shallow; significant discharge of interflow can originate from this layer.

Pumping groundwater from the SFL radically modifies flow patterns in the aquifer, as groundwater from the upper horizon, the saprolite, leaks vertically downward towards the pumped SFL and flow directions within the SFL can be drastically modified (Fig. 9b). The groundwater chemistry and ages are modified (rejuvenation; see for instance Roques et al. 2018), as the natural vertical water stratification described previously is altered. Incidently, mixing of subsurface groundwaters with deeper ones due to pumping enhances denitrification processes, where there are any (Roques et al. 2018).

Within a 50-km^2 granite watershed in Andrah Pradesh (now Telangana), India, Dewandel et al. (2012) evaluated the connectivity of the SFL fractures and aquifer compartmentalization in areas of about 650 × 650 m. However, the number of permeable fractures and their connectivity in the SFL decrease with depth (most of the fractures in granites are subhorizontal, see section 'Geological structure and hydrodynamic properties of weathering profiles'); then Guihéneuf et al. (2014) show that, depending on the elevation of the piezometric level, the aquifer can shift from a "watershed flow system" to an independent local flow system. Under high piezometric-level conditions, the interface including the bottom of the saprolite and the first flowing fractured zone in the upper part of the granite controls groundwater flow at "watershed-scale" (or at the scale of smaller areas: see Dewandel et al. 2012). Under low piezometric-level conditions, the aquifer is characterised by lateral compartmentalization due to decrease in the number of permeable fractures with depth and their connectivity. Then, individual compartments each exhibit a diameter of about 100 m only. This phenomenon, not presented in Fig. 9a,b, has important implications for

watershed hydrology, groundwater chemistry, aquifer vulnerability and pollutant transfer.

Operational hydrogeological applications based on this conceptual model

Several practical hydrogeological applications (and for applied geosciences) are derived from these concepts and the mapping methodology. This new genetic conceptual model of HRA leads to a revision of the methodologies used for characterizing the structure and functioning of such aquifers.

Another asset is the improvement of the efficiency of some of these methodologies, particularly geophysical methods. Two-dimensional electrical profiling now allows a rather precise imaging of the complete weathering profile (Belle et al. 2016, 2017; Soro et al. 2017). Magnetic resonance soundings allow estimation of HRA hydrodynamic parameters (specific yield and transmissivity; Vouillamoz et al. 2014; Wyns et al. 2004). The following strategy for siting a water well relies on these concepts.

Strategy for water-well siting in hard-rock aquifers

The strategy for siting a water borehole is improved and depends on the following cases:

1. Generally, where the SFL is not eroded, it will efficiently be tapped by vertical boreholes targeting the subhorizontal (in granite) or randomly dipping (in most metamorphic rocks) fractures of the SFL (see Fig. 1).
2. In some cases, where the SFL has been removed by erosion, or is unsaturated, it is more efficient to target a vertical fractured layer located along the walls of a subvertical discontinuity (Fig. 7), but avoiding its inner saprolite core, and large weathered corridors (described in section '"Deep vertical" discontinuities in the unweathered basement'; Arias et al. 2016; Belle et al. 2016, 2017).

In the first case (saturated SFL), the survey focuses on the SFL preserved from erosion, not clogged by weathering or diagenesis, with saturation (below the piezometric level). Vertical boreholes are used to reach the subhorizontal fractures of the granite SFL or the unevenly dipping fractures of the metamorphic rock SFL. The siting of hand-dug wells uses similar principles, looking for the coarse lower part of the saprolite and the underlying top of the SFL, which are rather easy to dig (Bakundukize et al. 2016).

In the second case (no or unsaturated SFL), techniques for well siting such as lineament analysis, geophysics and radon surveys (Lachassagne et al. 2001b; Reddy et al. 2006), can be used. As weathering is also the main driver of aquifer development in this context, linking open discontinuities to past or recent tectonic events and to recent or paleo stress-field data is not of interest, as indirectly shown by Holland and Witthüser (2011). This is because weathering develops along all heterogeneities whatever their orientation. Moreover, in most cases, regional plate-scale stresses do not influence fractures in the first hundreds of metres below the surface; topographic factors predominate (see references cited by Lachassagne et al. 2011).

Still in this second case (no or unsaturated SFL), inclined boreholes are more efficient than vertical ones at increasing the probability of crosscutting a vertical structure, to intersect it. Such a well-located inclined borehole will avoid cross cutting only the low-hydraulic-conductivity saprolite core of the structure and will cross cut its two permeable surroundings.

In both cases, as explained in the preceding (for the SFL in section 'Geological structure and hydrodynamic properties of weathering profiles'), the success of water-well siting also relies on the financial and technical feasibility of drilling several wells (at least 2 or 3) to account for the possible drilling of a first dry well (and eventually a second) that would (case 1) only have crosscut impervious fractures of the SFL or (case 2) only crosscut impervious fractures along the subvertical discontinuity.

Mapping hydrogeological potentialities and water-well siting in hard-rock aquifers

Water-borehole siting techniques in hard-rock aquifers, for population, agricultural and industrial water supply, have been developed based on the concepts and research outcomes summarised in the preceding. These rely on physical considerations about weathering and its hydrodynamic consequences on the SFL hydraulic conductivity (section 'Most favorable criteria and drivers for good aquifer properties') and on statistical and field observations (section 'Mapping hydrogeological potentialities and water-well siting at various scales: regional to country scale approach'). The SFL hydraulic conductivity is one of the main drivers of a borehole's productivity. Siting productive boreholes, with sufficient discharge threshold, is a challenge in HRA where many unsuccessful dry boreholes are drilled. The long-term exploitable discharge of a borehole or the sustainable abstraction from an aquifer relies on other parameters such as the available water resource. This issue is addressed further in this paper (section 'Quantitative management and modeling of HRA groundwater resources at the watershed scale: managed aquifer recharge').

Most favorable criteria and drivers for good aquifer properties

The mineralogy, texture and structure of HR influences the weathering and consequently the hydrodynamic properties of

the HRA. This has been described in detail in Lachassagne et al. 2014b, and is summarised in the following:

1. *Mineralogy*. Biotite is the most common mineral that is responsible for creating fractures in hard rocks during weathering. It is found in many plutonic rocks (granitoids) and metamorphic rocks (micaschists, paragneisses and orthogneisses). The abundance of biotite fosters the fracturing. White micas also swell during weathering, but later than biotite; the weathering of muscovite and K-felspar begins when the rock has already been transformed into sandy saprolite. Therefore, the weathering of muscovite plays no part in the fracturing of hard rocks. In some white mica-bearing rocks such as sericitoschists, the weathering of sericite can contribute to fracturing. Feldspars do not swell during weathering even if the transformation of plagioclase into clay minerals begins as early as the biotite transformation. In mafic and ultramafic rocks such as peridotites, weathering conduces swelling of olivine and pyroxene and consequently facilitates intense fracturing of the rock (Dewandel et al. 2005, 2017c; Rudge et al. 2010). Secondarily, pseudo-karstification may develop in such hard rocks below the saprolite cover mainly made up of limonite (Genna et al. 2005).
2. *Texture*. During weathering, the pressure caused by swelling minerals depends upon mineral size. Therefore, hard-rock fracturing is easier in coarse-grained rocks than in microgranular ones; hence, microgranites containing biotite are less fractured than granites.
3. *Structure*. During weathering, the swelling of biotite minerals occurs perpendicular to the cleavage. The layer spacing is changed from 10 Å to 14 Å as biotite is altered to hydrobiotite then to vermiculite. This is caused by the exchange of ions (K^+) initially between layers by larger, hydrated cations (Mg^{2+}, Na^+, Mn^{2+}, Ca^{2+}) and water molecules. Swelling pressure exerted perpendicular to cleavage and the resulting stress ellipsoid shape depend on the orientation of the minerals. Thus, the rock permeability tensor is dependent on the swelling mineral(s) orientation; see Lachassagne et al. 2014b for a detailed description and figures presenting the various cases summarized here:
    a. When swelling minerals are almost randomly oriented, as in plutonic rocks, the theoretical deformation ellipsoid is isotropic. Vertical stress increases until the lithostatic charge is offset, whereas horizontal stresses continue to increase. Horizontal tension joints are created when the difference between minor and major stress components reaches the elastic limit. The resulting reservoir properties (permeability, porosity) are good, and the main permeability component is horizontal.
    b. When the swelling minerals are vertically oriented (e.g. gneiss with vertical folitation), the deformation ellipsoid is anisotropic, with the main axis orthogonal to mineral orientation (i.e., horizontal); the maximum stress component has horizontal orientation, and the resulting tension joints are horizontal and generally largely open. The resulting reservoir properties (permeability, porosity) are good, and the major permeability component is horizontal.
    c. When the swelling minerals are horizontally oriented, the swelling potential is vertical, and the horizontal stress is slight. In this case, there are no or few open tension joints, but the rock acquires a horizontal laminated structure. The resulting reservoir properties are poorer.
    d. In metasedimentary folded rocks (such as schists, micaschists, gneisses) the orientation of swelling minerals varies laterally, and the bedding creates lithological preferential brittleness planes. Breaking joints are created in random directions.
4. *Synthesis*. For plutonic rocks, granular, biotite-bearing granites, granodiorites and diorites (as with unmetamorphosed gabbros) exhibit good hydrodynamic properties within their SFL. For metamorphic rocks, orthogneisses, paragneisses and micaschists can exhibit good hydrodynamic properties if their foliation dip is near-vertical, but poorer when foliation dip is near-horizontal. Consequently, biotite-rich rocks (such as biotite-granites, biotite-gneisses or micaschists) show a well-developed SFL, with a relatively high hydraulic conductivity and thick saprolite, whereas biotite-poor rocks such as leucogranites, are poorly weathered/fractured. This results in a granitic landscape where leucogranite intrusions in biotite-granite form relatively unweathered hills, tens of metres high, standing above the weathered and eroded biotite-granite cover. A similar landscape results from differential weathering of metamorphic rocks where unweathered quartzite ridges steeply emerge from flat weathered schists or micaschists. In granite-type rocks, a higher-hydraulic-conductivity SFL develops in coarse-grained rocks such as porphyric or pegmatitic granite, whereas fine-grained granites, like aplitic granites, develop a lower-hydraulic-conductivity SFL. In foliated rocks, the fracturing intensity is maximum where the foliation is subvertical, whereas it decreases and reaches a minimum where the foliation is subhorizontal. Peridotites, which are considered as HR by several authors, can form good aquifers; however, they show a dual aquifer behavior, pseudo-karstic and fractured (Dewandel et al. 2005, 2017c; Join et al. 2005; Jeanpert et al. 2019).

Mapping hydrogeological potentialities and water-well siting at various scales: regional to country scale approach

In many hard-rock aquifer studies, the blow discharge of a borehole measured during and on completion of drilling

has been regarded as a robust indicator of the local hydraulic conductivity/transmissivity of the aquifer, and thus of the SFL (or at least of the part of the SFL cross cut by the borewell). The blow discharge is, most of the time, obtained at the end (or during) drilling with a down-the-hole hammer. It consists of measuring the discharge of the well after a few minutes of air injection (to stabilize the discharge); the hammer is slightly lifted so that it is no longer in the position of drilling. The blow discharge is more rarely obtained with a specific device such as an air-lift system. The blow discharge is also regarded as a good indicator of the future exploitable discharge of the well, particularly for village water supply where (low) discharges of >0.5 m^3/h are required (Lenck 1977), and where the aquifer-scale water resource is not (yet) an issue. The depth to the base of the saprolite can also be measured with reasonable accuracy during drilling, by a geologist or hydrogeologist, or by the driller. It is determined accurately as there is always a strong hardness difference between the (unconsolidated) saprolite and the underlying hard SFL. The total drilled depth of a borehole is also accurately measured and recorded; however, sometimes, there can be some recurrences of this interface, notably when the top of the SFL comprises boulders (corestones).

These data (discharge, depth to the base of the saprolite, total depth of the well) are often reported and stored in national databases (Courtois et al. 2010). Statistics computed from these data, particularly those gathered in Africa during large village hydraulics programs, are used to infer, at regional scale, the hydrodynamic properties of the various lithologies underlying a study area (see for instance Lenck 1977). These statistical methodologies have been refined using the presented conceptual model (Courtois et al. 2010). In fact, the hydraulic conductivity of a borehole, or the blowing discharge, strongly correlates with the depth of the well below the base of the saprolite. The "linear discharge" (Courtois et al. 2010) is defined as the blowing discharge/the depth of the well below the base of the saprolite (Fig. 10). Then, (1) the boreholes that only cross-cut the saprolite have a low to nil discharge, and (2) the shallowest boreholes that reach the SFL cross-cut the more densely fractured part of the SFL and provide a higher linear discharge than the deeper ones that also cross-cut less- or unfractured levels.

The statistical processing of the linear discharge parameter, for each lithology, allows computation of two further important parameters (Courtois et al. 2010):

1. The thickness of the productive part of the SFL—in Burkina Faso for instance this thickness can be 35–40 m depending on the lithology (Fig. 10).
2. Hydrodynamical parameters such as statistical parameters about the potential discharge of the boreholes to be drilled in a given area: mean, median, standard deviation, percentage of "dry" boreholes below a discharge threshold, etc.

Such results have direct practical uses. In association with the thickness of the saprolite (Fig. 6b), the results provide an estimation of optimal borehole depth, i.e. the depth beyond which it is not necessary to drill, as the small gain in discharge does not justify the increased drilling cost. Hence, the results are of interest for planning (duration) and for assessing the financial cost of drilling campaigns (cumulative length amount and depth of the wells to be drilled, including numbers of "dry" boreholes) including the preliminary geophysical surveys that can also be precisely sized. They provide an estimated minimum depth for water wells necessary to cross the saprolite and reach the SFL, and as such can be used to evaluate the drilling constraints, i.e. the technical characteristics of the drilling rig and borewell equipment. Other applications can be inferred from the results such as mapping the mean discharge of boreholes at regional/country scale for different depths and correlating these results with economic parameters such as drilling costs, and other fields beyond hydrogeology such as town and country planning, soils engineering, the search for areas suitable for quarrying, etc.

Mapping hydrogeological potentialities and water-well siting at various scales: local scale

Such results at large scale are also of interest for local-scale hydrogeological projects. However, available data from wells may be insufficient to compute robust statistics. In that case, high-resolution mapping (with principles such as shown in Figs. 4 and 5) is needed for water-well siting. By also using information on land-use, land-ownership, conditions of access, etc., favorable zones for geophysical surveys and then exploratory drillings can be selected (Fig. 11).

At a local scale, geophysical methods, especially 2D electrical geophysical methods, rarely delineate junctions between lithologies or enable identification of lithologies (Belle et al. 2016, 2017). Nevertheless, they are very efficient at characterising the structure of the weathering profile (they can identify the saprolite, the SFL, their thickness and geometry, etc.).

The typical response in granites is, from top to bottom (Belle et al. 2016, 2017; Soro et al. 2017; Fig. 12):

1. High resistivity, up to several hundreds to 1,000 ohm-m; occurrence of (unsaturated) saprolite and/or, where preserved, iron or bauxitic duricrust.
2. Lower resistivity, down to a few tens of ohm-m or lower; this indicates clayey saprolite and/or the saturated clayey saprolite.

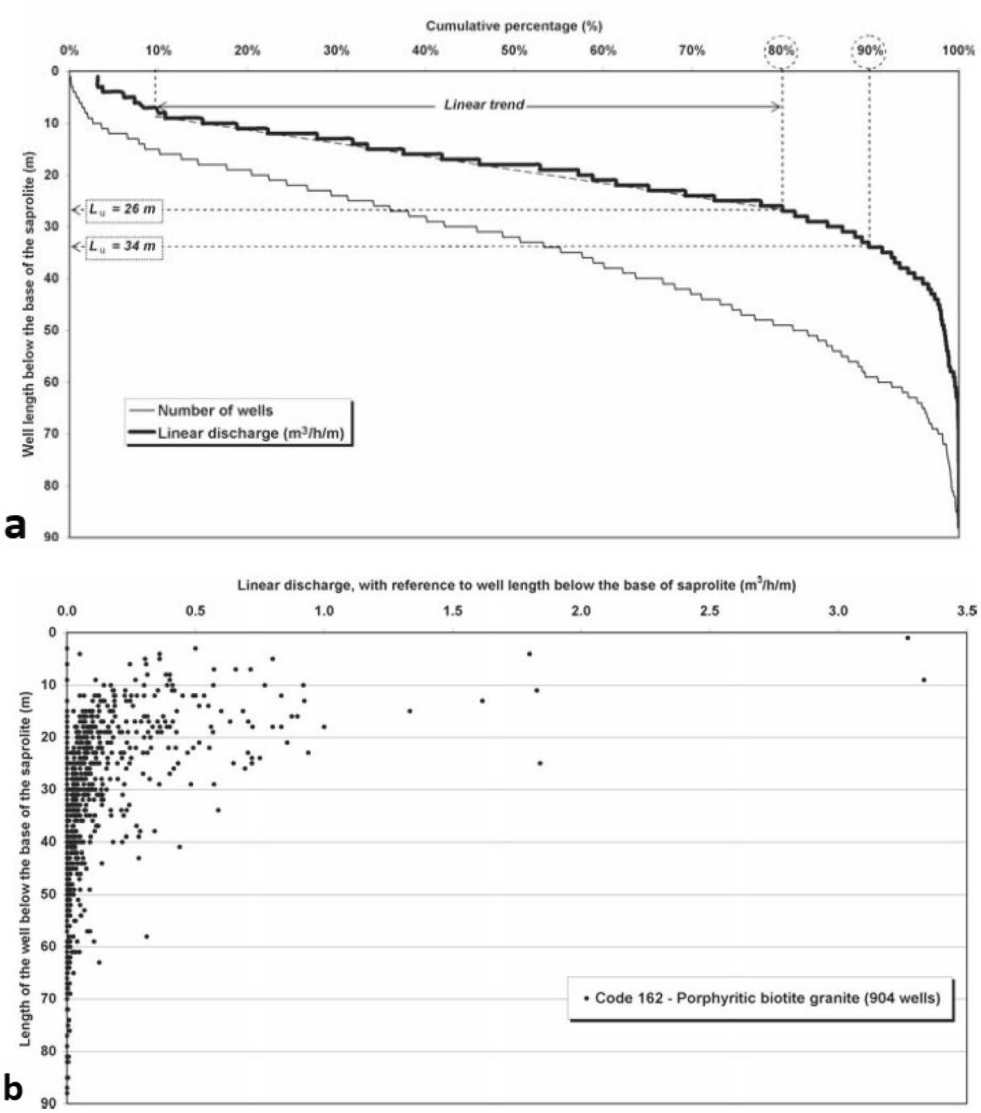

Fig. 10 **a** Cumulative percentage of linear discharge (X axis, %; see the definition of the linear discharge in the text) as a function of the length of the well below the base of the saprolite (Y axis, m), to estimate the thickness of the fractured layer for the porphyritic biotite granite in Burkina Faso (from Courtois et al. 2010) **b** Data set used to prepare **a** ($N = 904$ wells; X axis = linear discharge ($m^3/h/m$), Y axis: length of the well below the base of the saprolite (m); from Courtois et al. 2010). With permission from Wiley

3. Steadily increasing resistivity within the sandy saprolite (isalterite) and then within the SFL. The fractured layer resistivity is often below 600 ohm-m, and locally can be less than 100 ohm-m. Where present and thick enough, the laminated-layer resistivity is identified by a local increase in the resistivity (up to 600 ohm-m), and then a decrease (to that of the SFL; Belle et al. 2016, 2017), within this increasing trend from the low resistivity saprolite to the SFL and its substratum (Fig. 12).
4. The highest resistivity (up to more than 10,000 ohm-m) is reached within the unweathered/unfractured rock.

The preceding text (section "'Deep vertical' discontinuities in the unweathered basement) describes large deep low-permeability structures that show resistivity less than 150–100 ohm-m (Belle et al. 2016 and 2017; Fig. 12).

As described in section 'Geological structure and hydrodynamic properties of weathering profiles', Dewandel et al. (2012, 2017b, 2017c) developed a method to map the spatial variations of hydrodynamic properties (hydraulic conductivity, specific yield) at the aquifer scale. Mapping can also use electrical geophysical data (Chandra et al. 2008).

Vouillamoz et al. (2014) used magnetic resonance soundings (MRS) to estimate the specific yield and the transmissivity of HRA in Bénin, as otherwise determined from pumping tests (same scale). The MRS water content is about twice the specific yield. They then propose two linear relationships for calculating the specific yield from MRS water content, with an uncertainty of 10%, and from the pore-size parameter, with an uncertainty of 20%. The latter identifies nondrainable MRS water content and, thus, low groundwater reserve. Aquifer transmissivity is estimated using MRS with an accuracy of 70%.

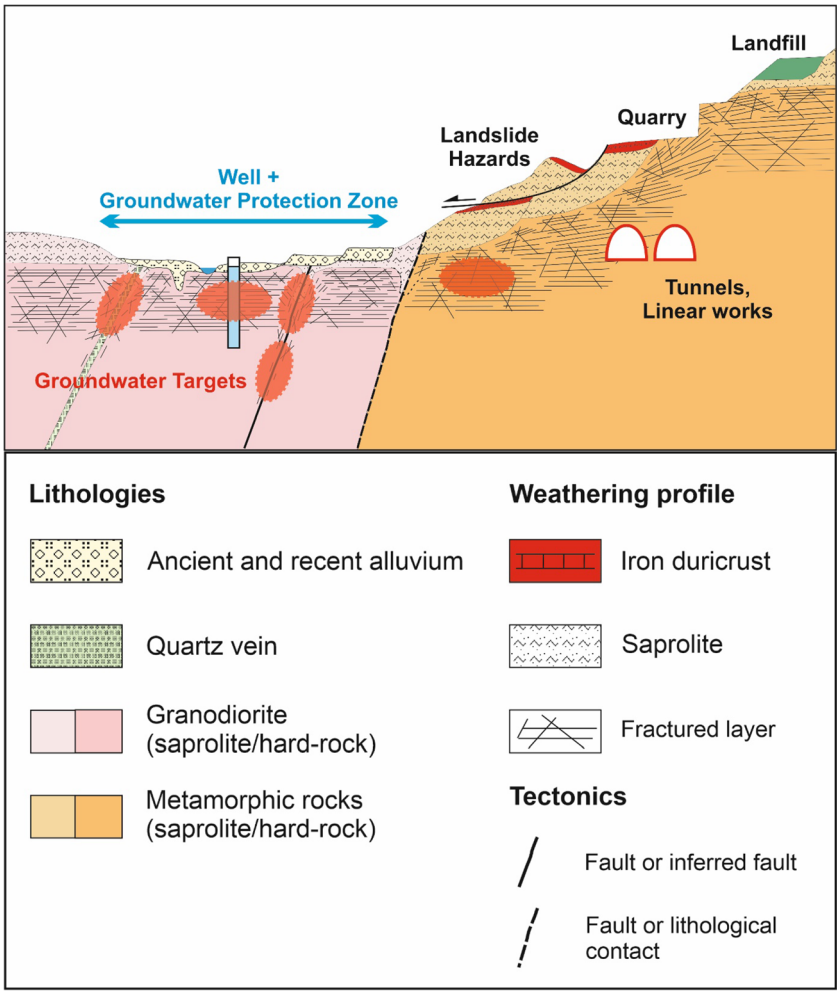

Fig. 11 Various practical applications of a high-resolution mapping of the weathering cover at the local scale (see Fig. 4 for the legend and section 'Geological structure and hydrodynamic properties of weathering profiles'; from Courtois et al. 2003). The five orange ellipses represent potential targets, of various interest, for water-well siting

High-resolution mapping (with principles such as shown in Figs. 4 and 5) is used for the delineation of groundwater protection zones, and also for other applications such as the location of landfill sites on the upper saprolite where rock weathering forms a clayey layer, and the location of rock quarries with a minimum cover cap, preferably where the weathering profile is eroded or at the boundary between successive weathering profiles (Fig. 11; section 'Other applications in applied geosciences').

Delineating groundwater watersheds and piezometric mapping in HRA

Piezometric heads in HRA well mimic the surface topography (see also section 'Hydrogeological functioning of HR aquifers: hydrochemistry'). Consequently, delineating groundwater watersheds from topographic data (groundwater watershed = surface-water watershed) is possible.

Using topographic data, and location and elevation of perennial stream water levels, with piezometric measurements, allows computation of piezometric maps (Wyns et al. 2004; Yao et al. 2015), even with limited data. Methodologies for the optimisation of piezometric networks in HRA have been proposed by Zaidi et al. (2007).

Quantitative management and modeling of HRA groundwater resources at the watershed scale: managed aquifer recharge

Several methods have been developed for water resources management of HRA using, as input or calibration data (Dewandel et al. 2010, 2012, 2017b): (1) the concept of stratiform layers, (2) the relative homogeneity of HRA hydrodynamic properties at a scale of a few 100 m, beyond the local scale of a single well (see for instance Dewandel et al. 2014, 2018; Lachassagne et al. 2016) that can be dry (Dewandel et al. 2012), (3) the decrease of the specific yield with depth, as well as (4) the spatial variations of the specific yield.

Maréchal et al. (2006) show that the combined use of water-table-fluctuation and groundwater-budget methods is appropriate at the watershed scale and relevant for this purpose; for instance, Chinnasamy et al. (2018) also

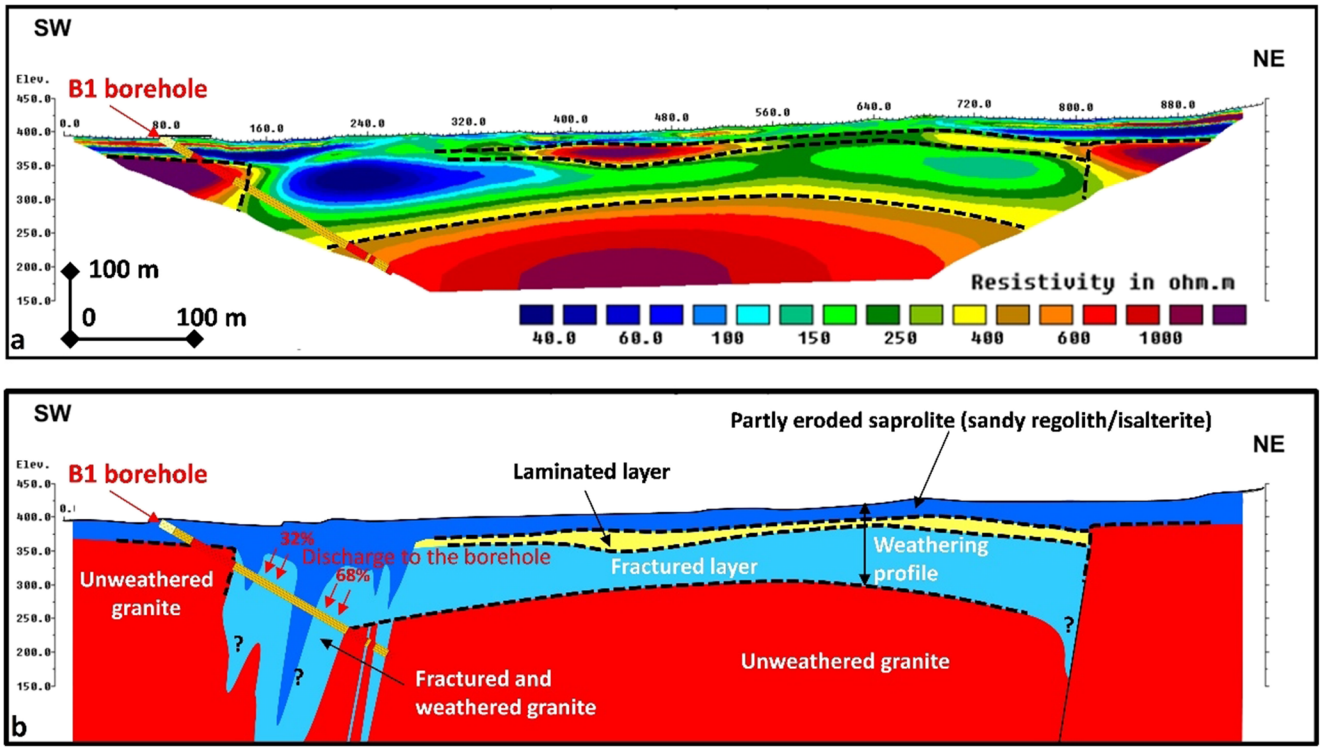

Fig. 12 **a** Example of an electrical resistivity tomography geophysical profile in granitic weathered HR and **b** its hydrogeological interpretation. Saint-Galmier, Loire Department, Massif Central, France (from Belle et al. 2017, modified). Pole-dipole array with "standard horizontal" (STDH) inversion parameters

use this combined method. Similar methods have been applied to overexploited HRA in India (Maréchal et al. 2006; Dewandel et al. 2007b, 2010), even through use of soil and water assessment tools (SWAT models) that are applicable in such a hydrogeological context where groundwater vertical fluxes prevail over regional lateral flow at km-scale (Ferrant et al. 2014; Perrin et al. 2012). Such models can be used for water resources mapping and simulation of scenarios such as land use changes, changes in water uses and climate change. Remote sensing data are also crucial to provide cheap and efficient input or calibration data for these models (see for instance Ferrant et al. 2017 for the context of Indian HRA).

Lachassagne et al. (2016) forecast daily piezometric variations in a weathered-fractured metamorphic aquifer pumped by a well, taking account of its discharge and pumped aquifer characteristics, including recharge. They developed a simple lumped reservoir model (1) based on the hydrodynamic parameters, and shape and size of the aquifer diagnosed from the early months of time series discharge/piezometric level (D/PL) data from that well, and (2) calibrated from the D/PL time series data. The computed aquifer recharge time series appears realistic.

The demonstration that HRA are constituted by rather homogeneous layers (saprolite and SFL) at least at the scale of a few hundreds of meters allows their deterministic mathematical modelling with "classical models" similar to those used for sedimentary aquifers modelling (see for instance Lachassagne et al. 2001a; Leray et al. 2013; Baiocchi et al. 2014; Durand et al. 2017; Dickson et al. 2018). This was performed for water resources evaluation and to propose management scenarios.

Decision support tools have been developed from these methodologies (Dewandel et al. 2007b, 2011; Mizam et al. 2019; Lachassagne et al. 2016), and strategies built, some integrating climate change impacts (Ferrant et al. 2014; Mizam et al. 2019; Fig. 13).

The evaluation of managed aquifer recharge (MAR) from percolation tanks is assessed by Perrin et al. (2012), Boisson et al. (2014), Alazard et al. (2016), and Nicolas et al. (2019). Recharge is delayed in the aquifer due to slow groundwater flow; the unsaturated saprolite acts as a buffer to aquifer recharge. Due to the compartmentalization of the aquifer, and despite a large number of pumping boreholes surrounding the tank, the radius of influence of the percolation tank is small, and only a few boreholes benefit from the tank artificial recharge. The characteristics (geometry, hydraulic conductivity) of the SFL fractures drive the lateral propagation of the aquifer recharge (Nicolas et al. 2019). MAR appears to be beneficial for groundwater quality, particularly with respect to reducing fluoride contamination (Pauwels et al. 2015; Pettenati et al. 2014).

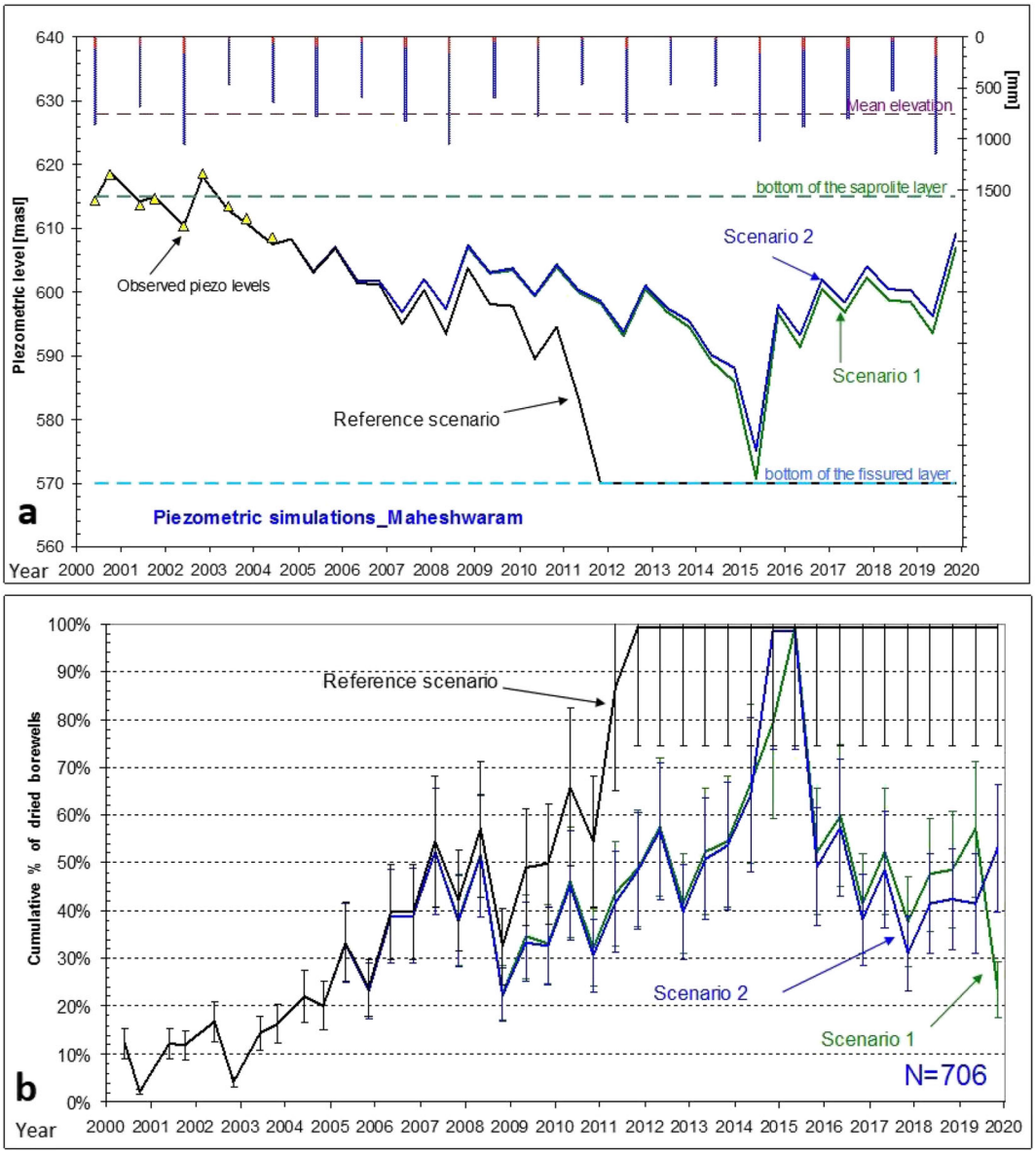

Fig. 13 Example of long-term resource management simulation at the watershed scale, Maheswaram, Andhra Pradesh (now Telangana), India: **a** mean piezometric level; **b** number of dried wells (Dewandel et al. 2010). With permission from Wiley

Assessing HRA groundwater reserves from watershed to regional scales

These new concepts allow assessment of HRA groundwater reserves from the watershed to the regional scale through combined use of the 3D geometry of the weathering profile and the vertical distribution of effective porosity determined by magnetic resonance soundings (MRS) (Wyns et al. 2002, 2004; Baltassat et al. 2005; Vouillamoz et al. 2014, 2015) or its evaluation using 3D aquifer parameter regionalization methods (Dewandel et al. 2012, 2017b; Mizan et al. 2019).

Magnetic resonance soundings allow determination of the mean effective porosity of the three parts of the aquifer: saprolite, upper fractured layer, and lower fractured layer. For a given lithology, several MRS are used to determine the mean porosity of each layer. The saturated thickness of each layer, multiplied by the porosity, gives the water content for each cell expressed in water height (Figs. 14 and 15). The total groundwater reserve is given by the addition of the water height of the three layers of the aquifer. Vouillamoz et al. (2015) estimate groundwater storage in Benin metamorphic rocks to be between 200 and 1,200 mm. At a 270-km^2 study area located in Brittany, France, underlain by Hercynian plutonic and metamorphic rocks (Wyns et al. 2004), values range between 100 and 1,500 mm—as proposed by Vouillamoz et al. (2015); the results from Wyns et al. (2004) were divided by 2 to account for calibration by pumping tests.

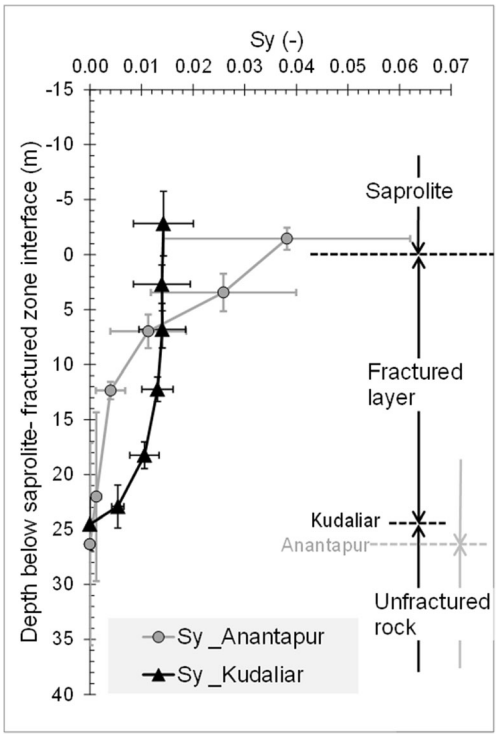

Fig. 14 Average specific yield (Sy) in the weathering profile for the Anantapur and Kudaliar watersheds, Andhra Pradesh (now Telangana), India; bars depict standard deviations (from Dewandel et al. 2017b). With permission from Wiley

The most recent and advanced methods for estimating groundwater reserves probably come from the use of groundwater-budget and water-table-fluctuation techniques, combined with satellite remote sensing methods (Dewandel et al. 2012, 2017b; Ferrant et al. 2017; see also section 'Geological structure and hydrodynamic properties of weathering profiles'). Such methods were combined with the knowledge of the weathering profile geometry and geostatistical approaches for regionalizing. These methods allow evaluation of the 3D distribution of the effective porosity at the aquifer scale (Dewandel et al. 2012, 2017b) and the recharge, along with its spatial distribution (Mizan et al. 2019). Some recent studies (e.g., Chinnasamy et al. 2018) do not consider the vertical structure of the HRA and find less precise values of specific yield, which may yield inaccurate forecasts. Figure 14 shows, for two large watersheds (more than 700 km^2), how the effective porosity varies on average with depth into the weathering profile. Then, with data on water-table depth, it allows computation of the groundwater reserve at the watershed scale, and also establishes scarcity and vulnerability maps with respect to pumping, for assessing the areas most vulnerable to groundwater overexploitation (Fig. 15).

Protecting and restoring HRA groundwater resources, groundwater quality modelling, and contaminant transfer

As discussed in the preceding (section 'Hydrogeological functioning of HR aquifers: hydrochemistry', dealing with HRA piezometry), the delineation of groundwater protection zones for water wells relies on knowledge of the geometry and hydrodynamic properties of the exploited HR aquifers (particularly the presence and extension of the clayey saprolite that can prevent local (pollutants) infiltration), and thereby ensure groundwater protection (section 'Hydrogeological functioning of HR aquifers: hydrochemistry' dealing with recharge of HRA). Knowledge of geometry and hydrodynamics also yields more precise piezometric maps that can be used to identify flow systems and subwatersheds (section 'Delineating groundwater watersheds and piezometric mapping in HRA').

Evaluation of HRA groundwater reserves (section 'Assessing HRA groundwater reserves from watershed to regional scales'), taking into account the recharge of the aquifer, allows for calculation of the average residence time of groundwater in the aquifer, and the duration of residence of non-point-source pollutants such as diffuse nitrate contamination. For the sites studied in Benin, Vouillamoz et al. (2015) compute a "buffer capacity" of 6 ± 4 years.

The methodologies developed for the quantitative management of HRA groundwater resources (section 'Quantitative management and modeling of HRA groundwater resources at the watershed scale: managed aquifer recharge') can be applied to the management of groundwater quality. Perrin et al. (2011b) designed a lumped reservoir model to simulate long-term piezometric and solute concentrations in a 53-km^2 watershed in India. They then reproduced chloride concentrations and show that, in that case study in a semiarid context and overexploitation for irrigation, solute recycling will induce long-term aquifer salinisation. In fact, evapotranspiration impacts the quality of the return flow from irrigation, through a higher concentration of salts in recharged water and soils, and a higher enrichment in stable isotopes of the water molecules that are successfully used to quantify such processes (Négrel et al. 2011). The same evapotranpiration processes induce fluoride concentration in aquifers prone to this geochemical influence (Pettenati et al. 2013; Pauwels et al. 2015). Paddy fields show large irrigation return flows (Dewandel et al. 2007a), but a higher rate of evaporation at the surface, due to their inundation, than other crops (Négrel et al. 2011). Perrin et al. (2012) simulated the impact of various scenarios on the groundwater quality (e.g., higher pumping

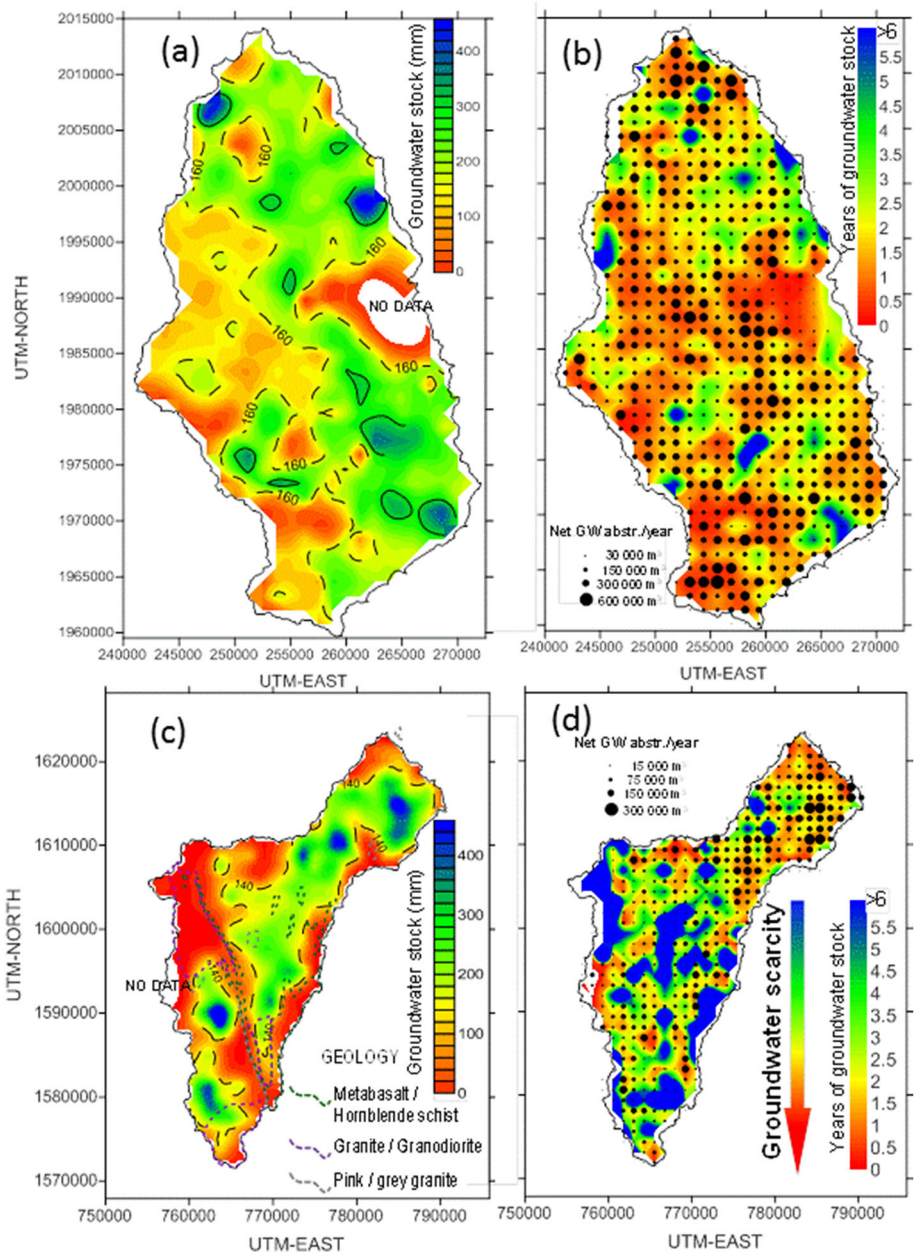

Fig. 15 Examples of groundwater storage maps (in water height) for **a** Kudaliar watershed and **c** Anantapur (Andhra Pradesh, now Telangana) watershed, India; for Anantapur the main geological unit, gneiss, is not shown. Maps showing groundwater scarcity and vulnerability to overpumping of the aquifer for **b** Kudaliar and **d** Anantapur. Cell size 1,250 × 1,250 m. The size of black dots (Fig. 16b,d) corresponds to the amount of net groundwater abstraction (in m^3/year). From Dewandel et al. (2017b). With permission from Wiley

rates, decrease in rainfall, increase in evapotranspiration, etc.).

The methodologies developed for the regionalisation and mapping of HRA hydrodynamic parameters such as specific yield and hydraulic conductivity (Dewandel et al. 2012, 2017b), are of interest in terms of contaminant transport evaluation and modelling in such a hydrogeological context. Taylor et al. (2010) provide some estimates of saprolite dispersivity, and Guihéneuf et al. (2017) characterize the solute transport properties of the fractured layer of an Indian granite aquifer; they notably confirm that non-Fickian dispersion dominates.

Computing the drainage discharge and the hydrogeological and hydrological impacts of tunnels drilled in HR

The drainage discharge and the surface impacts of shallow tunnels in HR were studied in the 4,000-m-long Violay Tunnel, France (Lachassagne et al. 2014c; Fig. 16). Hydrogeological impacts include piezometric drawdown in wells and drying up of springs; hydrological impacts include the decrease of stream discharge. These impacts have been forecasted applying the HRA concepts presented in this review paper. The depth of the tunnel was 0–300 m below the

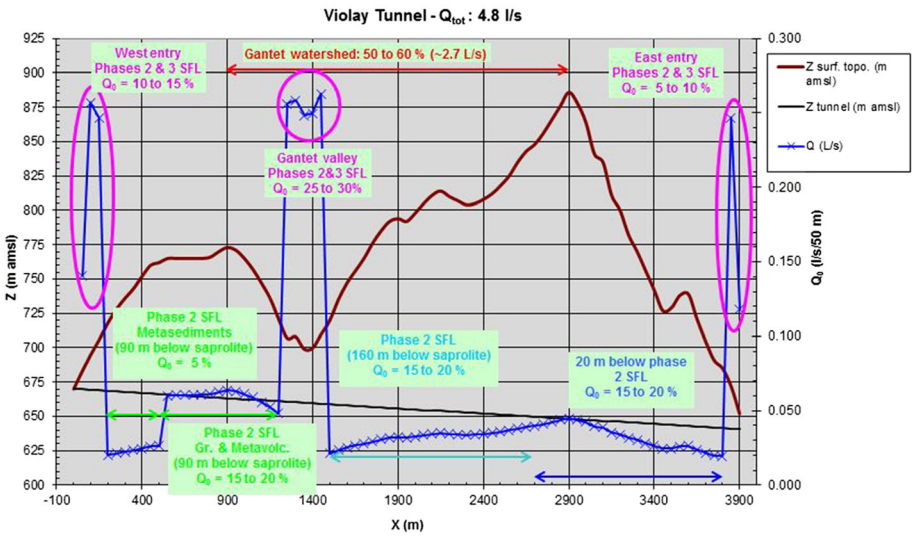

Fig. 16 Violay (Loire Department, Massif Central, France) tunnel computed discharge Q_0 (blue crosses - L/s/50 m of tunnel) according to the lithology, the weathering grade and the depth of the tunnel (black line) below the topographic surface (brown profile). The highest-discharge areas (purple circles) are located at both entries of the tunnel, and in the Gantet River Valley, where the tunnel crosscuts the SFL of the weathering phases 2 and 3. The other parts of the tunnel are either within or below the phase 2 SFL. In the first kilometre of the tunnel, the discharge change is due to a lithological change. This computation provides a 4.8 L/s discharge for the whole tunnel. The estimated surface-water loss in the Gantet watershed is about 2.7 L/s (in red). From Lachassagne et al. (2014c)

ground surface, and consequently within and below the weathering profile.

The following computations were performed (Lachassagne et al. 2014c):

1. Characterisation of the location of the tunnel within or below the various layers constituting the weathering profile, which was polyphased and locally deepened by various deep veins and ancient faults.
2. Measurement of the steady-state groundwater discharge in existing tunnels in the same area and associated lithologies (and their location within the weathering profiles).
3. The analytical solutions for tunnel inflow.

The actual discharge of the now drilled tunnels, within the predicted range, validates the efficacy of the methodology. The impact of the recent shallow weathering profile is evidenced near the entrances of the tunnel (Fig. 16), as already shown by several other authors, even if they did not all relate this to a weathering profile. In a more subtle way, discharge variations related to the depth of the tunnel below the base of the saprolite are also shown (see the right section of Fig. 16).

Thermal and mineral water

Most of the thermal and mineral water occurrences, including carbo-gaseous ones, do emerge from outcropping hard rocks. In fact, a sedimentary cover may hinder upwards vertical flows (water, gas) from deep origin. Additionally, most thermal and mineral springs are a mix of such deep waters (and gas in some cases) and groundwater from near-surface aquifers. Then, interaction within the superficial HRA between these two types of waters is common; in the superficial HRA, water from the overlying saprolite mixes with deep thermo-mineral water (Maréchal et al. 2014).

The edges of grabens (Dewandel et al. 2017a) often show well-preserved weathering profiles, as the dominant process during the creation of the basin was sedimentation at these locations, not erosion. These profiles can form thick capacitive aquifers, fed by upwelling deep mineral water rising from a few fractures (notably the graben normal faults), and by downflowing low-mineralisation waters from the HRA (Fig. 17). The SFL of the HRA acts as the main aquifer and it is easily reached by production boreholes.

Generalisation of these observations reveals strong opposite characteristics between (1) low-inertia crystalline thermo-mineral (carbo-gaseous) hydrosystems without a subsurface reservoir (as the weathering profile was eroded) and (2) high-inertia ones as already just described. The former generally provide highly mineralized water, but at a very low discharge (Ledoux et al. 2016), whereas the latter provide more diluted water, but with a much higher discharge (Dewandel et al. 2017a).

The chemical reactions involved in the weathering process of rock fracturing are exothermic. This exothermic weathering process has been invoked as a possible hypothesis to explain geothermal anomalies (water warmer than expected) observed in some HRA, notably in the western part of France (Wyns et al. 2015), in quite shallow wells (about 100 m deep). However, Vasseur and Lachassagne (2019) demonstrated that

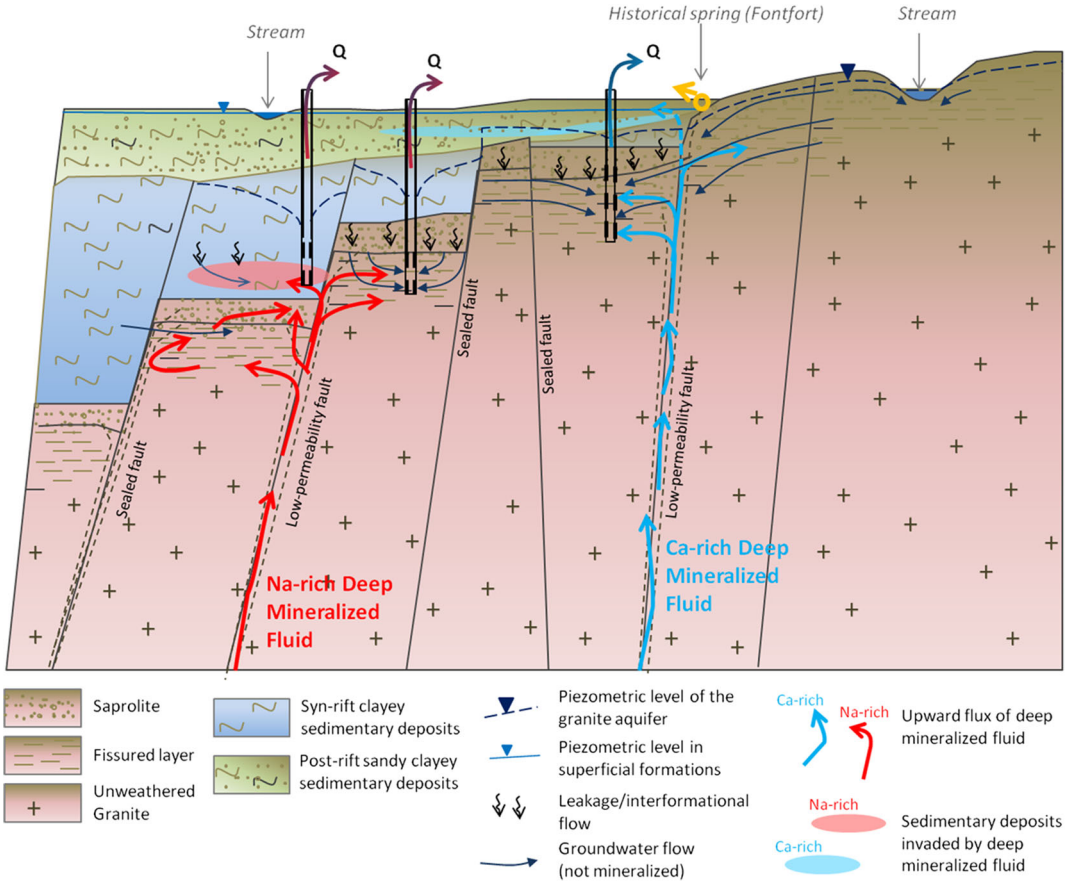

Fig. 17 Conceptual model of a carbo-gaseous mineral hydrosystem (Saint-Galmier, Loire, France) where the fractured layer of the weathering profile constitutes the main aquifer (from Dewandel et al. 2017a). With permission from Elsevier

this exothermic process of weathering has no significant geothermal impact at the aquifer scale, and at the weathering timescale. In fact, heat diffusion and advection quickly evacuate the small amount of generated heat, and so the temperature cannot increase. Thus, the process of HR weathering cannot explain these geothermal anomalies. More classical explanations such as the local upwards flow from deep fractures, should then be invoked.

Other applications in applied geosciences

Prior to improvement and development for hydrogeological application, weathering profile concepts have indicated geodynamic evolution (Wyns 1991) within geological mapping (Wyns et al. 1998), and aided radioactive-waste-storage safety analysis (Wyns 1991, 1997). These concepts can help locate and identify faults in HR, as layers and interfaces in the weathering profile, to reveal the location and throw of faults (Cho et al. 2002; Lachassagne et al. 2001c).

Applications have been developed in the investigation of soil and rock mechanics to forecast mechanical properties for: the subsoil burial of electrical and telephonic cable networks at 1/25,000 to 1/100,000 scale (Wyns et al. 1999, 2005); quarrying in HR (Rocher et al. 2003; Fig. 11); evaluation of the thickness of the cover cap; the determination of optimal geo-mechanic quality of the materials, etc. Future applications will include preliminary surveys for highways and railways. The HRA conceptual model has been applied to hydrocarbon reservoirs in crystalline rocks (Wyns 2015), and it is acknowledged that some hydrocarbon reservoirs are found in HRA (see for instance Riber et al. 2017 and Tan et al. 2017).

Conclusion and perspectives

The hydraulic conductivity and storativity of HR are mostly inherited from weathering processes. Consequently, HRA develop mostly within the first 100 m below ground surface. Where not partially or totally eroded, they comprise: (1) a capacitive but rather low-permeability unconsolidated weathered layer, the saprolite, located immediately above (2) the permeable stratiform fractured layer. To a lesser extent, weathering and hydraulic conductivity develop deeper in the unweathered rock, at the periphery of or within preexisting geological discontinuities (lithological contacts, joints, dykes, veins, etc.).

The demonstration and recognition of this conceptual model allowed development of a comprehensive corpus of applied methodologies in hydrogeology and geology, which are described in this review paper: water well siting, mapping hydrogeological potentialities from the local to the country scale, quantitative management, modeling and protection of HRA groundwater resources, even in thermal and mineral aquifers, computing the discharge of tunnels, quarrying of HR, etc.

The properties of such HRA have been described and understood in granites, and several applications have been developed. Metamorphic rocks, being more complex and heterogeneous, will require more detailed characterisation in the future using applications developed for plutonic rocks.

One of the other challenges with respect to both plutonic and metamorphic rocks is to develop geophysical method(s) able to identify if (or where) the fractures of the SFL are permeable, from the surface, i.e. locally down to >50 m deep. This would be of great interest for water borehole siting. In fact, 3D high-resolution permeable-fracture imaging has already been achieved (see for instance Robinson et al. 2016), but only from drillings, and not from the surface.

Acknowledgements

This paper synthesizes more than 20 years of research projects on hard-rock aquifers, involving several scientists and collaborators; many of these projects were undertaken in France and India. Beyond the references cited in this paper, the list of all these contributors would be too long; however, we hope that they will all recognize themselves and will accept these acknowledgements.

The leader of this issue's topical collection on hard-rock aquifers, Uwe Tröger, and an anonymous reviewer, are also warmly thanked for their careful review, which helped improve the manuscript before its formal submission to *Hydrogeology Journal*. We thank Prof. Maurizio Barbieri and two more anonymous reviewers who also formally reviewed this paper.

We also want to thank the organizers of the International Conference on Groundwater in Fractured Rocks (GwFR'2017) organized by the International Association of Hydrogeologists (IAH) 'Network on Fractured Rock Hydrogeology' and the Portuguese and Spanish Chapters of IAH in Chaves, Portugal, in June 2017, and notably Raquel Sousa who encouraged us to write this review paper after our Conference's oral presentations (notably the following presentation: Lachassagne et al. 2017). As this paper was submitted in November 2017, it was later completed with additional recent references in August 2019, during its revision; recommendations from the reviewer were received in June 2019 and the revision completed in September 2019, before the last formal submission to *Hydrogeology Journal* in August 2020.

References

Acworth RI (1987) The development of crystalline basement aquifers in a tropical environment. Q J Eng Geol 20:265–272. https://doi.org/10.1144/GSL.QJEG.1987.020.04.02

Alazard M, Boisson A, Maréchal JC, Perrin J, Dewandel B, Schwarz T, Pettenati M, Picot-Colbeaux G, Kloppman W, Ahmed S (2016) Investigation of recharge dynamics and flow paths in a fractured crystalline aquifer in semi-arid India using borehole logs: implications for managed aquifer recharge. Hydrogeol J 24(1):35–57

Alle C, Descloitres M, Vouillamoz JM, Yalo N, Lawson FMA, Adihou C (2017) Why 1D electrical resistivity techniques can result in inaccurate siting of boreholes in hard rock aquifers and why electrical resistivity tomography must be preferred: the example of Benin, West Africa. J African Earth Sci 139(2018):341–353. https://doi.org/10.1016/j.jafrearsci.2017.12.007

Anovitz LM, Cheshire MC, Hermann RP, Guc X, Sheets JM, Brantley SL, Cole DR, Ilton ES, Mildner DFR, Gagnon C, Allard LF, Littrell KC (2021) Oxidation and associated pore structure modification during experimental alteration of granite. Geochim Cosmochim Acta 292(2021):532–556. https://doi.org/10.1016/j.gca.2020.08.016

Arias D, Pando L, Lopez-Fernandez C, Diaz-Diaz LM, Rubio-Ordonez A (2016) Deep weathering of granitic rocks: a case of tunnelling in NW Spain. Catena 137(2016):572–580. https://doi.org/10.1016/j.catena.2015.10.026

Armandine Les Landes A, Aquilina L, Davy P, Vergnaud-Ayraud V, Le Carlier C (2015) Timescales of regional circulation of saline fluids in continental crystalline rock aquifers (Armorican Massif, western France). Hydrol Earth Syst Sci 19:1413–1426

Achtziger-Zupancik P, Loew S, Mariéthoz G (2017) A new global database to improve predictions of permeability distribution in crystalline rocks at site scale. J Geophys Res Solid Earth 122:3513–3539. https://doi.org/10.1002/2017JB014106

Babaye MSA, Orban P, Ousmane B, Favreau G, Brouyère S, Dassargues A (2019) Characterization of recharge mechanisms in a Precambrian basement aquifer in semi-arid south-west Niger. Hydrogeol J 27:475–491. https://doi.org/10.1007/s10040-018-1799-x

Baiocchi A, Dragoni W, Lotti F, Piscopo V (2014) Sustainable yield of fractured rock aquifers: the case of crystalline rocks of Serre Massif (Calabria, southern Italy). In: Fractured rock hydrogeology. IAH Selected Papers, no. 20. CRC, Boca Raton, FL, pp 79–97

Baiocchi A, Lotti F, Piscopo V (2016) Occurrence and flow of groundwater in crystalline rocks of Sardinia and Calabria (Italy): an

overview of current knowledge Acque Sotterranee. Ital J Groundw 5(1). https://doi.org/10.7343/as-2016-195

Bakundukize C, Mtoni Y, Martens K, Van Camp M, Walraevens K (2016) Poor understanding of the hydrogeological structure is a main cause of hand-dug wells failure in developing countries: a case study of a Precambrian basement aquifer in Bugesera region (Burundi). J African Earth Sci 121(2016):180–199. https://doi.org/10.1016/j.jafrearsci.2016.05.025

Baltassat JM, Legchenko A, Ambroise B, Mathieu F, Lachassagne P, Wyns R, Mercier JL, Schott JJ (2005) Magnetic resonance sounding (MRS) and resistivity characterisation of a mountain hard rock aquifer: the Ringelbach Catchment, Vosges Massif, France. Near Surf Geophys 3(4):267–274

Bauer H, Bessin P, Saint-Marc P, Châteauneuf JJ, Bourdillon C, Wyns R, Guillocheau F (2016) The Cenozoic history of the Armorican Massif: new insights from the deep CDB1 borehole (Rennes Basin, France). C R Geosci 348(5):387–397. https://doi.org/10.1016/j.crte.2016.02.002

Belle P, Lachassagne P, Mathieu F, Barbet C, Bonneval F (2016) Nouvelles avancées dans l'interprétation géologique et hydrogéologique des profils de tomographie électrique en contexte de socle granitique et métamorphique [Recent progress in the geological and hydrogeological interpretation of ERT profiles in granitic and metamorphic crystalline rocks]. Géologues 191(2016):13–17

Belle P, Lachassagne P, Mathieu F, Brisset N, Barbet C, Bonneval F, Gourry JC (2017) Geological and hydrogeological interpretation of hard rock weathering profil from electrical tomography. In: Ofterdinger U, Macdonald AM, Comte JC, Young ME (eds) Groundwater in fractured bedrock environments. Geol Soc Lond Spec Publ 479. https://doi.org/10.1144/SP479.7

Boisson A, Baïsset M, Alazard M, Perrin J, Villesseche D, Dewandel B, Kloppmann W, Chandra S, Picot-Colbeaux G, Sarah S, Ahmed S, Maréchal JC (2014) Comparison of surface and groundwater balance approaches in the evaluation of managed aquifer recharge structures: case of a percolation tank in a crystalline aquifer in India. J Hydrol 519(2014):1620–1633. https://doi.org/10.1016/j.jhydrol.2014.09.022

Boisson A, Guihéneuf N, Perrin J, Bour O, Dewandel B, Dausse A, Viossanges M, Ahmed S, Maréchal JC (2015) Determining the vertical evolution of hydrodynamic parameters in weathered and fractured south Indian crystalline-rock aquifers: insights from a study on an instrumented site. Hydrogeol J 23(4):757–773. https://doi.org/10.1007/s10040-014-1226-x

Braun J, Mercier J, Guillocheau F, Robin C (2016) A simple model for regolith formation by chemical weathering. J Geophys Res Earth Surf 121:2140–2171. https://doi.org/10.1002/2016JF003914

Cai Z, Ofterdinger U (2016) Analysis of groundwater-level response to rainfall and estimation of annual recharge in fractured hard rock aquifers, NW Ireland. J Hydrol 535(2016):71–84. https://doi.org/10.1016/j.jhydrol.2016.01.066

Caine JS, Evans JP, Forster CB (1996) Fault zone architecture and permeability structure. Geology 24(11):1025–1028

Chabaux F, Viville D, Lucas Y, Ackerer J, Ranchoux C, Bosia C, Pierret MC, Labasque T, Aquilina L, Wyns R, Lerouge C, Dezaye C, Négrel P (2017) Geochemical tracing and modeling of surface and deep water–rock interactions in elementary granitic watersheds (Strengbachand Ringelbach CZOs, France). Acta Geochim 36(3):363–366. https://doi.org/10.1007/s11631-017-0163-5

Chambel A (2014) Outcrop groundwater prospecting, drilling and well construction in hard rocks in semi-arid regions. In: Fractured rock hydrogeology. IAH Selected Papers, no. 20. CRC, Boca Raton, FL, pp 61–78

Chandra S, Ahmed S, Ram A, Dewandel B (2008) Estimation of hard rock aquifers hydraulic conductivity from geoelectrical measurements: a theoretical development with field application. J Hydrol 357:218–227. https://doi.org/10.1016/j.jhydrol.2008.05.023

Chandra S, Ahmed Sh, Auken E, Pedersen JB, Singh A, Verma SK (2016) 3D aquifer mapping employing airborne geophysics to meet India's water future. The Leading Edge 35(9):770–774. https://doi.org/10.1190/tle35090770.1

Chardon D, Grimaud JL, Beauvais A, Bamba O (2018) West African lateritic pediments: landform-regolith evolution processes and mineral exploration pitfalls. Earth-Sci Rev 179(2018):124–146. https://doi.org/10.1016/j.earscirev.2018.02.009

Charlier JB, Lachassagne P, Ladouche B, Cattan P, Moussa R, Voltz M (2011) Structure and hydrogeological functioning of an insular tropical humid andesitic volcanic watershed: a multi-disciplinary experimental approach. J Hydrol 398(2011):155–170

Chilton PJ, Foster SSD (1995) Hydrogeological characterisation and water-supply potential of basement aquifers in tropical Africa. Hydrogeol J 3(1):36–49

Chilton PJ, Smith-Carington AK (1984) Characteristics of the weathered basement aquifer in Malawi in relation to rural water supplies. In: Challenges in African Hydrology and Water Resources (Proceedings of the Harare Symposium, July 1984). IAHS Publ. no. 144, IAHS, Wallingford, UK

Chinnasamy P, Maheswari B, Dillon P, Purohitd R, Dashorad Y, Sonie P, Dashora R (2018) Estimation of specific yield using water table fluctuations and cropped area in a hardrock aquifer system of Rajasthan, India. Agric Water Manag 202(2018):146–155. https://doi.org/10.1016/j.agwat.2018.02.016

Chirindja FJ, Dahlin T, Juizo D (2017) Improving the groundwater-well siting approach in consolidated rock in Nampula Province, Mozambique. Hydrogeol J 25:1423–1435. https://doi.org/10.1007/s10040-017-1540-1

Cho M, Choi Y-S, Ha KC, Kee WS, Lachassagne P, Wyns R (2002) Paleoweathering covers in Korean hard rocks: a methodology for mapping their spatial distribution and the thickness of their constituting horizons—applications to identify brittle deformation and to hard rock hydrogeology. KIGAM Bull (Korean Institute of Geoscience and Mining Bulletin) 6(2):12–25

Cho M, Choi Y, Ha K, Kee W, Lachassagne P, Wyns R (2003) Relationship between the permeability of hard rock aquifers and their weathering, from geological and hydrogeological observations in South Korea. International Association of Hydrogeologists IAH Conference on Groundwater in fractured rocks, Prague, 15–19 September 2003

Chou P-Y, Lin J-J, Hsu S-M, Lo H-C, Chen P-J, Ke C-C, Lee W-R, Huang C-C, Chen N-C, Wen H-Y, Lee F-M (2014). Characterising the spatial distribution of transmissivity in the mountainous region: results from watersheds in central Taiwan. In: Fractured rock hydrogeology. IAH Selected Papers, no. 20. CRC, Boca Raton, FL, pp 114–127

Chuang P-Y, Chia Y, Liou Y-H, Teng M-H, Liu C-Y (2016) Characterization of preferential flow paths between boreholes in fractured rocks using a nanoscale zero-valent iron tracer test. Hydrogeol J 24:1651–1662. https://doi.org/10.1007/s10040-016-1426-7

Compaore G, Lachassagne P, Pointet Th, Travi Y (1997) Evaluation du stock d'eau des altérites: expérimentation sur le site granitique de Sanon (Burkina Faso) [Assessment of the alterite water stock: experiment on the granite site of Sanon (Burkina Faso)]. Hard Rock Hydrosystems (Proceedings of Rabat Symposium S2, May 1997). IAHS Publ. no. 241, IAHS, Wallingford, UK, pp 37–46

Comte JC, Cassidy R, Nitsche J, Ofterdinger U, Pilatova K, Flynn R (2012) The typology of Irish hard-rock aquifers based on an integrated hydrogeological and geophysical approach. Hydrogeol J 20(8):1569–1588. https://doi.org/10.1007/s10040-012-0884-9

Courtois N, Lachassagne P, Weng P, Theveniaut H, Wyns R, Joseph B, Laporte P (2003) Détermination de secteurs potentiellement favorables pour la recherche d'eau souterraine à Cacao (Guyane) [Identification of potentially favorable sectors for groundwater

exploration in Cacao (Guyana)]. Report BRGM/RM-52758-FR, BRTGM, Orléans, France

Courtois N, Lachassagne P, Wyns R, Blanchin R, Bougaïre FD, Some S, Tapsoba A (2010) Large-scale mapping of hard-rock aquifer properties applied to Burkina Faso. Ground Water 48(2):269–283

David K, Liu T, David V (2014) Use of several different methods for characterising a fractured rock aquifer, case study Kempfield, New South Wales, Australia. In: Fractured rock hydrogeology. IAH Selected Papers, no. 20. CRC, Boca Raton, FL, pp 308–327

Davies J, Robins N, Cheney C (2014) Similarities of groundwater occurrence in weathered and fractured crystalline basement aquifers in the Channel Islands and in Zimbabwe. In: Fractured rock hydrogeology. IAH Selected Papers, no. 20. CRC, Boca Raton, FL, pp 47–60

de Montety V, Aquilina L, Labasque T, Chatton E, Fovet O, Ruiz L, Fourré E, de Dreuzy JR (2018) Recharge processes and vertical transfer investigated through long-term monitoring of dissolved gases in shallow groundwater. J Hydrol 560(2018):275–288

Dewandel B, Lachassagne P, Qatan A (2004) Spatial measurements of stream baseflow, a relevant method for aquifer characterization and permeability evaluation: application to a hard-rock aquifer, the Oman ophiolite. Hydrol Process 18(17):3391–3400. https://doi.org/10.1002/hyp.1502

Dewandel B, Lachassagne P, Boudier F, Al Hattali S, Ladouche B, Pinault JL, Al-Suleimani Z (2005) A conceptual model of the structure and functioning of the Oman ophiolite hard-rock aquifer through a pluridisciplinary and multiscale approach. Hydrogeol J 13:708–726

Dewandel B, Lachassagne P, Wyns R, Maréchal JC, Krishnamurthy NS (2006) A generalized 3-D geological and hydrogeological conceptual model of granite aquifers controlled by single or multiphase weathering. J Hydrol 330(1–2):260–284

Dewandel B, Gandolfi JM, de Condappa D, Ahmed S (2007a) An efficient methodology for estimating irrigation return flow coefficients of irrigated crops at watershed and seasonal scale. Hydrol Process. https://doi.org/10.1002/hyp.6738

Dewandel B, Gandolfi JM, Zaidi FK, Ahmed S, Subrahmanyam K (2007b) A decision support tool with variable agro-climatic scenarios for sustainable groundwater management in semi-arid hard-rock areas. Curr Sci 92(8):1093–1102

Dewandel B, Perrin J, Ahmed S, Aulong S, Hrkal Z, Lachassagne P, Samad M, Massuel S (2010) Development of a decision support tool for managing groundwater resources in semi-arid hard rock regions under variable water demand and climatic conditions. Hydrol Process 24:27884–22797

Dewandel B, Lachassagne P, Chandra S, Zaidi FK (2011) Conceptual hydrodynamic model of a geological discontinuity in hard rock aquifers: example of quartz reef in granitic terrain in South India. J Hydrol 405:474–487

Dewandel B, Maréchal J-C, Bour O, Ladouche B, Ahmed S, Chandra S, Pauwels H (2012) Upscaling and regionalizing hydraulic conductivity and efficient porosity at watershed scale in crystalline aquifers. J Hydrol 416-471:83–97

Dewandel B, Aunay B, Maréchal JC, Roques C, Bour O, Mougin B, Aquilina L (2014) Analytical solutions for analysing pumping tests in a sub-vertical and anisotropic fault zone draining shallow aquifers. J Hydrol 509(2014):115–131. https://doi.org/10.1016/j.jhydrol.2013.11.014

Dewandel B, Alazard M, Lachassagne P, Bailly-Comte V, Couëffé R, Grataloup S, Ladouche B, Lanini S, Maréchal JC, Wyns R (2017a) Respective roles of the weathering profile and the tectonic fractures in the structure and functioning of a crystalline thermomineral carbo-gaseous aquifer. J Hydrol 547(2017):690–707. https://doi.org/10.1016/j.jhydrol.2017.02.028

Dewandel B, Caballero Y, Perrin J, Boisson A, Dazin F, Ferrant S, Chandra S, Maréchal J-C (2017b) A methodology for regionalizing 3-D effective porosity at watershed scale in crystalline aquifers. Hydrol Process 31(12):2277–2295. https://doi.org/10.1002/hyp.11187

Dewandel B, Jeanpert J, Ladouche B, Join JL, Maréchal JC (2017c) Inferring the heterogeneity, transmissivity and hydraulic conductivity of crystalline aquifers from a detailed water-table map. J Hydrol 550(2017):118–129. https://doi.org/10.1016/j.jhydrol.2017.03.075

Dewandel B, Lanini S, Lachassagne P, Maréchal J-C (2018) A generic analytical solution for modelling pumping tests in wells intersecting fractures. J Hydrol 559:89–99. https://doi.org/10.1016/j.jhydrol.2018.02.013

Dickson NEM, Comte JC, Koussoube Y, Ofterdinger U, Vouillamoz JM (2018) Analysis and numerical modelling of large-scale controls on aquifer structure and hydrogeological properties in the African basement (Benin, West Africa). Geol Soc Lond Spec Publ 479. https://doi.org/10.1144/SP479.2

Durand V, Deffontaines B, Léonardi V, Guérin R, Wyns R, Marsily de G, Bonjour J-L (2006) A multidisciplinary approach to determine the structural geometry of hard-rock aquifers. Application to the Plancoët migmatitic aquifer (NE Brittany, W France). Bull Soc Géol France 177: 227–237

Durand V, Léonardi V, de Marsily G, Lachassagne P (2017) A new quality-of-fit criterion to quantify the specific yield in a two-layer hard-rock aquifer model. J Hydrol 551(2017):328–339. https://doi.org/10.1016/j.jhydrol.2017.05.013

Ferrant S, Caballero Y, Perrin J, Gascoin S, Dewandel B, Aulong S, Dazin F, Ahmed S, Marechal JC (2014) Projected impacts of climate change on farmers' extraction of groundwater from crystalline aquifers in South India. Nat Sci Rep 4:3697. https://doi.org/10.1038/srep03697

Ferrant S, Selles A, Le Page M, Herrault PA, Pelletier C, Al-Bitar A, Mermoz S, Gascoin S, Bouvet A, Saqalli M, Dewandel B, Caballero Y, Ahmed S, Maréchal JC, Kerr Y (2017) Detection of irrigated crops from Sentinel-1 and Sentinel-2 data to estimate seasonal groundwater use in South India. Remote Sens 2017(9):1199. https://doi.org/10.3390/rs9111119

Figueiredo B, Tsang C-F, Niemi A, Lindgren G (2016) The state-of-art of sparse channel models and their applicability to performance assessment of radioactive waste repositories in fractured crystalline formations. Hydrogeol J 24:1607–1622. https://doi.org/10.1007/s10040-016-1415-x

Foster S (2012) Hard-rock aquifers in tropical regions: using science to inform development and management policy. Hydrogeol J 20: 659–672

Francés AP, Lubczynski MW, Roy Y, Santos FAM, Mahmoudzadeh Ardekani MR (2014) Hydrogeophysics and remote sensing for the design of hydrogeological conceptual models in hard rocks: Sardón catchment (Spain). J Appl Geophys 110(2014):63–81. https://doi.org/10.1016/j.jappgeo.2014.08.015

Genna A, Maurizot P, Lafoy Y, Augé T (2005) Role of karst in the nickeliferous mineralisations of New Caledonia. C R Geosci 337: 367–374

Guihéneuf N, Boisson A, Bour O, Dewandel B, Perrin J, Dausse A, Viossanges M, Chandra S, Ahmed S, Maréchal JC (2014) Groundwater flows in weathered crystalline rocks: impact of piezometric variations and depth-dependent fracture connectivity. J Hydrol 511(2014):320–334. https://doi.org/10.1016/j.jhydrol.2014.01.061

Guihéneuf N, Bour O, Boisson A, Le Borgne T, Becker MW, Nigon B, Wajiduddin M, Ahmed S, Maréchal JC (2017) Insights about transport mechanisms and fracture flow channeling from multiscale observations of tracer dispersion in shallow fractured crystalline rock. J Contaminant Hydrol. https://doi.org/10.1016/j.jconhyd.2017.09.003

Hart D (2016) A comparison of fracture transmissivities in granite water wells before and after hydrofracturing. Hydrogeol J 24:21–33. https://doi.org/10.1007/s10040-015-1315-5

Hasenmueller HE, Gub X, Weitzman JN, Adams TS, Stinchcomb GE, Eissenstat DM, Drohan PJ, Brantley SL, Kaye JP (2017) Weathering of rock to regolith: the activity of deep roots in bedrock fractures. Geoderma 300(2017):11–31. https://doi.org/10.1016/j.geoderma.2017.03.020

Hill SM (1996) The differential weathering of granitic rocks in Victoria, Australia. J Aust Geol 16:271–276

Holland M, Witthüser KT (2011) Evaluation of geologic and geomorphologic influences on borehole productivity in crystalline bedrock aquifers of Limpopo Province, South Africa. Hydrogeol J 19:1065–1083. https://doi.org/10.1007/s10040-011-0730-5

Ingebritsen S, Gleeson T (2017) Crustal permeability. Hydrogeol J. 25: 2221–2224. https://doi.org/10.1007/s10040-017-1663-4

Jahns RH (1943) Sheet structure in granites, its origin and use as a measure of glacial erosion in New England. J Geol 51(2):71–98

Jeanpert J, Iseppi M, Adler PM, Genthon P, Sevin B, Thovert J-F, Dewandel B, Join J-L (2019) Fracture controlled permeability of ultramafic basement aquifers: inferences from the Koniambo Massif, New Caledonia. Eng Geol 256(2019):67–83. https://doi.org/10.1016/j.enggeo.2019.05.006

Join JL, Robineau B, Ambrosi JP, Costis C, Colin F (2005) Groundwater in ultramafic mined massifs of New Caledonia. C R Geosci 337: 1500–1508

Krasny J (1996) Hydrogeological environment in hard rocks: an attempt at its schematizating and terminological considerations. In: Proceedings of the First Workshop on Hard Rock Hydrogeology of the Bohemian Massif. Acta Univ Carolinae Geol 40(2):115–122

Lachassagne P, Ahmed S, Golaz C, Maréchal J-C, Thiery D, Touchard, F, Wyns R (2001a) A methodology for the mathematical modelling of hard-rock aquifers at catchment scale based on the geological structure and the hydrogeological functioning of the aquifer. In: XXXI IAH Congress New Approaches Characterizing Groundwater Flow. Hard Rock Hydrogeology session, AIHS, Munich, Germany

Lachassagne P, Pinault J-L, Laporte P (2001b) Radon-222 Emanometry: a relevant methodology for water well siting in hard rock aquifer. Water Resour Res 37(12):3131–3148

Lachassagne P, Wyns R, Bérard P, Bruel T, Chéry L, Coutand T, Desprats J-F, Le Strat P (2001c) Exploitation of high-yield in hard-rock aquifers: downscaling methodology combining GIS and multicriteria analysis to delineate field prospecting zones. Ground Water 39(4):568–581

Lachassagne P, Wyns R, Dewandel B (2011) The fracture permeability of hard rock aquifers is due neither to tectonics, nor to unloading, but to weathering processes. Terra Nova 23:145–161

Lachassagne P, Aunay B, Frissant N, Guilbert M, Malard A (2014a) High-resolution conceptual hydrogeological model of complex basaltic volcanic islands: a Mayotte, Comoros, case study. Terra Nova 26(4):307–321

Lachassagne P, Dewandel B, Wyns R (2014b) The conceptual model of weathered hard rock aquifers and its practical applications. In: Fractured rock hydrogeology. IAH Selected Papers, no. 20. CRC, Boca Raton, FL, pp 13–46

Lachassagne P, Maréchal JC, Bienfait P, Lacquement F, Lamotte C (2014c) Computing the water inflows discharge and assessing the impacts of tunnels drilled in Hard Rocks IAEG XII Congress, Torino 2014. Eng Geol Soc Territory 3:595–599. https://doi.org/10.1007/978-3-319-09054-2_119

Lachassagne P, Barbet B, Dewandel B (2016) Reverse modeling: a simple and robust method for modeling and forecasting the piezometric level/discharge of a pumping well—a case study in a Hard Rock Aquifer. Proceedings of the 43rd IAH Congress, Montpellier, France, 25th–29th September 2016

Lachassagne P, Dewandel B, Wyns R (2017) The conceptual model of weathered hard rock aquifers. application to their survey, management, modelling and protection. International Conference on Groundwater in Fractured Rocks (GwFR'2017) organized by the Network on Fractured Rock Hydrogeology and the Portuguese and Spanish Chapters of the International Association of Hydrogeologists (IAH), 5–7 June, Chaves, Portugal (oral presentation)

Leblanc MJ, Favreau G, Massuel S, Tweed OS, Loireau M, Cappelaere B (2008) Land clearance and hydrological change in the Sahel: SW Niger. Glob Planet Chang 61(2008):135–150. https://doi.org/10.1016/j.gloplacha.2007.08.011

Le Borgne T, Bour O, de Dreuzy J-R, Davy P, Touchard F (2004) Equivalent mean flow models for fractured aquifers: insights from a pumping tests scaling interpretation. Water Resour Res 40:12

Le Borgne T, Bour O, Paillet FL, Caudal J-P (2006) Assessment of preferential flow path connectivity and hydraulic properties at single-borehole and cross-borehole scale in a fractured aquifer. J Hydrol 328:347–359

Ledoux E, Xiao H, Terrisse JF, Lachassagne P (2016) Deterministic modelling of the Vals-les-Bains carbo-gaseous natural mineral hydrosystem and analysis of sensitivity to changes in land use and water management practices, chap 3.2. In: Lachassagne P, Lafforgue M (eds) Forest and the water cycle: quantity, quality, management. Cambridge Scholars, Cambridge, UK, pp 266–291

Lenck P-P (1977) Données nouvelles sur l'hydrogéologie des régions à substratum métamorphique ou éruptif: enseignements tirés de la réalisation de 900 forages en Côte d'Ivoire [New data on the hydrogeology of regions with a metamorphic or eruptive substratum: lessons learned from the construction of 900 boreholes in Côte d'Ivoire]. C R Acad Sci Paris 285:497–500

Leray S, de Dreuzy JR, Bour O, Bresciani E (2013) Numerical modeling of the productivity of vertical to shallowly dipping fractured zones in crystalline rocks. J Hydrol 481(2013):64–75. https://doi.org/10.1016/j.jhydrol.2012.12.014

Mandl G (2005) Rock joints: the mechanical genesis. Springer, Berlin

Maréchal J-C, Ahmed S (2003) Dark zones are human-made. Down to Earth 12(4):54

Maréchal JC, Sarma MP, Ahmed Sh, Lachassagne P (2002) Establishment of earth tide effect on water-level fluctuations in an unconfined hard rock aquifer using spectral analysis. Curr Sci 83(1), 10 July 2002

Maréchal J-C, Dewandel B, Subrahmanyam K (2004) Use of hydraulic tests at different scales to characterize fracture network properties in the weathered-fractured layer of a hard rock aquifer. Water Resour Res 40(11):17

Maréchal JC, Dewandel B, Ahmed S, Galeazzi L, Zaidi FK (2006) Combined estimation of specific yield and natural recharge in a semi-arid groundwater basin with irrigated agriculture. J Hydrol 329(1–2):281–293

Maréchal JC, Lachassagne P, Ladouche B, Dewandel B, Lanini S, Le Strat P, Petelet-Giraud E (2014) Structure and hydrogeochemical functioning of a sparkling natural mineral water system determined using a multidisciplinary approach: a case study from southern France. Hydrogeol J 22:47–68. https://doi.org/10.1007/s10040-013-1073-1

Maurice L, Taylor RG, Tindimugaya C, MacDonald AM, Johnson P, Kaponda A, Owor M, Sanga H, Bonsor HC, Darling WG, Gooddy D (2018) Characteristics of high-intensity groundwater abstractions from weathered crystalline bedrock aquifers in East Africa. Hydrogeol J 27:459. https://doi.org/10.1007/s10040-018-1836-9

Meyzonnat G, Barbecot FL, Corcho-Alvarado JA, Tognelli A, Zeyen H, Mattei A, McCormack R (2018) High-resolution wellbore temperature logging combined with a borehole-scale heat budget: conceptual and analytical approaches to characterize hydraulically active fractures and groundwater origin. Geofluids 2018, 9461214. https://doi.org/10.1155/2018/9461214

Michel JP, Fairbridge RW (1992) Dictionary of earth sciences/ Dictionnaire des sciences de la terre. McGraw-Hill, New York, 304 pp

Mizan SA, Dewandel B, Selles A, Ahmed S, Caballero Y (2019) A simple groundwater balance tool to evaluate the three-dimensional specific yield and the two-dimensional recharge: application to a deeply weathered crystalline aquifer in southern India. Hydrogeol J. https://doi.org/10.1007/s10040-019-02026-8

Monod B, Regard V, Carcone J, Wyns R, Christophoul F (2016) Postorogenic planar palaeosurfaces of the Central Pyrenees: weathering and neotectonic records. C R Geosci 348(3–4):184–193 https://doi.org/10.1016/j.crte.2015.09.005

Muchingami I, Chuma C, Gumbo C, Hlatywayo D, Mashingaidze R (2019) (2019). Review: approaches to groundwater exploration and resource evaluation in the crystalline basement aquifers of Zimbabwe. Hydrogeol J 27:915–928. https://doi.org/10.1007/s10040-019-01924-1

Négrel P, Pauwels H, Dewandel B, Gandolfi JM, Mascré C, Ahmed S (2011) Understanding groundwater systems and their functioning through the study of stable water isotopes in a hard-rock aquifer (Maheshwaram watershed India). J Hydrol 397(2011):55–70. https://doi.org/10.1016/j.jhydrol.2010.11.033

Neves M, Morales N (2007) Well productivity controlling factors in crystalline terrains of southeastern Brazil. Hydrogeol J 15(3):471

Nicolas M, Bour O, Selles A, Dewandel B, Bailly-Comte V, Chandra S, Ahmed S, Maréchal JC (2019) Managed aquifer recharge in fractured crystalline rock aquifers: impact of horizontal preferential flow on recharge dynamics. J Hydrol 573(2019):717–732. https://doi.org/10.1016/j.jhydrol.2019.04.003

Oliva P, Viers J, Dupré B (2003) Chemical weathering in granitic environments. Chemical Geol 202(3–4):225–256

Owen R, Maziti A, Dahlin T (2007) The relationship between regional stress field, fracture orientation and depth of weathering and implications for groundwater prospecting in crystalline rocks. Hydrogeol J 15(7):1231

Pauwels H, Négrel P, Dewandel B, Perrin J, Mascré C, Roy S, Ahmed S (2015) Hydrochemical borehole logs characterizing fluoride contamination in a crystalline aquifer (Maheshwaram India). J Hydrol 525(2015):302–312. https://doi.org/10.1016/j.jhydrol.2015.03.017

Perrin J, Ahmed S, Hunkeler D (2011a) The role of geological heterogeneities and piezometric fluctuations on groundwater flow and chemistry in hard-rock, southern India. Hydrogeol J 19(6):1189–1200. https://doi.org/10.1007/s10040-011-0745-y

Perrin J, Mascré C, Pauwels H, Ahmed S (2011b) Solute recycling: an emerging threat to groundwater quality in southern India. J Hydrol 398(1–2):144–154

Perrin J, Ferrant S, Massuel S, Dewandel B, Maréchal JC, Aulong S, Ahmed S (2012) Assessing water availability in a semi-arid hard-rock regions watershed of southern India using a semi-distributed model. J Hydrol 460–461(2012):143–155

Pettenati M, Perrin J, Pauwels H, Ahmed S (2013) Simulating fluoride evolution in groundwater using a reactive multicomponent transient transport model: application to a crystalline aquifer of southern India. Appl Geochem 29(2013):102–116 https://doi.org/10.1016/j.apgeochem.2012.11.001

Pettenati M, Picot-Colbeaux G, Thiéry D, Boisson A, Alazard M, Perrin J, Dewandel B, Maréchal J-C, Ahmed S, Kloppmann W (2014) Water quality evolution during managed aquifer recharge (MAR) in Indian crystalline basement aquifers: reactive transport modeling in the critical zone. Procedia Earth Planet Sci 10(2014):82–87. https://doi.org/10.1016/j.proeps.2014.08.016

Place J, Géraud Y, Diraison M, Herquel G, Edel JB, Bano M, Le Garzic E, Walter B (2015) Structural control of weathering processes within exhumed granitoids: compartmentalisation of geophysical properties by faults and fractures. J Struct Geol 84:102–119. https://doi.org/10.1016/j.jsg.2015.11.011

Pollard D, Aydin A (1988) Progress in understanding jointing over the past one hundred years. Geol Soc Am Bull 100:1181–1204

Reddy DV, Sukhija BS, Nagabhushanam P, Reddy GK, Kumar D, Lachassagne P (2006) Soil gas radon emanometry: a tool for delineation of fractures for groundwater in granitic terrains. J Hydrol 329(1–2):186–195

Riber L, Dypvik H, Sorlie R (2017) Comparison of deeply buried paleoregolith profiles, Norwegian North Sea, with outcrops from southern Sweden and Georgia, USA: implications for petroleum exploration. Palaeogeogr Palaeoclimatol Palaeoecol 471(2017):82–95 https://doi.org/10.1016/j.palaeo.2017.01.043

Robinson J, Slater L, Johnson T, Shapiro A, Tiedeman C, Ntarlagiannis D, Johnson C, Day-Lewis F, Lacombe P, Imbrigiotta T, Lane J (2016) Imaging pathways in fractured rock using three-dimensional electrical resistivity tomography. Groundwater 54(2):186–201. https://doi.org/10.1111/gwat.12356

Rocher P, Mishellany A, Wyns R, Lacquement F, Gobron N, Greffier G, Germain Y (2003) Identification et caractérisation des ressources en matériaux de substitution aux granulats alluvionnaires dans le département du Puy-de-Dôme: la zone des Combrailles [Identification and characterization of resources for substitute materials for alluvial aggregates in the Puy-de-Dôme department: the Combrailles area]. Report BRGM/RP52706-FR, BRGM, Orléans, France, 97 pp

Roques C, Aquilina L, Bour O, Maréchal JC, Dewandel B, Pauwels H, Labasque T, Vergnaud-Ayraud V, Hochreutener R (2014a) Groundwater sources and geochemical processes in a crystalline fault aquifer. J Hydrol 519(2014):3110–3128. https://doi.org/10.1016/j.jhydrol.2014.10.052

Roques C, Bour O, Aquilina L, Dewandel B, Leray S, Schroetter J-M, Longuevergne L, Le Borgne T, Hochreutener R, Labasque T, Lavenant N, Vergnaud-Ayraud V, Mougin B (2014b) Hydraulic behavior of a deep sub-vertical fault in crystalline basement and relationships with surrounding compartments. J Hydrol 509(2014):42–54

Roques C, Bour O, Aquilina L, Dewandel B (2016) High-yielding aquifers in crystalline basement: insights about the role of fault zones, exemplified by Armorican Massif, France. Hydrogeol J 24(8):2157–2170. https://doi.org/10.1007/s10040-016-1451-6

Roques C, Aquilina L, Boisson A, Vergnaud-Ayraud V, Labasque T, Longuevergne L, Laurencelle M, Dufresne A, de Dreuzy JR, Pauwels H, Bour O (2018) Autotrophic denitrification supported by biotite dissolution in crystalline aquifers: (2) transient mixing and denitrification dynamic during long-term pumping. Sci Total Environ 619–620(2018):491–503. https://doi.org/10.1016/j.scitotenv.2017.11.104

Royne A, Jamveit B, Matheiesen J, Malthe-Sorenssen A (2008) Controls on rock weathering rates by reaction-induced hierarchical fracturing. Earth Planet Sci Lett 275:364–369

Rudge JF, Kelemen PB, Spielgelman M (2010) A simple model of reaction-induced cracking applied to serpentinization and carbonation of peridotite. Earth Planet Sci Lett 291(2010):215–227. https://doi.org/10.1016/j.epsl.2010.01.016

Sander P (1997) Water-well siting in hard-rock areas: identifying promising targets using a probabilistic approach. Hydrogeol J 5(3):32

Sanford WE (2017) Estimating regional-scale permeability-depth relations in a fractured-rock terrain using groundwater-flow model calibration. Hydrogeol J 25:405–419. https://doi.org/10.1007/s10040-016-1483-y

Setlur N, Sharp JM, Hunt BB (2019) Crystalline-rock aquifer system of the Llano Uplift, central Texas, USA. Hydrogeol J 27:2431–2446

Soro DD, Koita M, Biaou CA, Outoumbe E, Vouillamoz J-M, Yacouba H, Guérin R (2017) Geophysical demonstration of the absence of correlation between lineaments and hydrogeologically useful fractures: case study of the Sanon hard rock aquifer (central northern Burkina Faso). J African Earth Sci 129:842–852

Tan P, Oberhardt N, Dypvik H, Riber L, Ferrel REJ (2017) Weathering profiles and clay mineralogical developments, Bornholm, Denmark. Marine Petrol Geol 80(2017):32–48. https://doi.org/10.1016/j.marpetgeo.2016.11.017

Taylor R, Howard K (2000) A tectono-geomorphic model of the hydrogeology of deeply weathered crystalline rock: evidence from Uganda. Hydrogeol J 8(3):279–294

Taylor RG, Howard K (1999) Lithological evidence for the evolution of weathered mantels in Uganda by tectonically controlled cycles of deep weathering and stripping. Catena 35(1):65–94

Taylor R, Tindimugaya C, Barker J, Macdonald D, Kulabako R (2010) Convergent radial tracing of viral and solute transport in gneiss saprolite. Ground Water 48(2):284–294

Theveniaut H, Freyssinet P (1999) Paleomagnetism applied to lateritic profiles to assess saprolite and duricrust formation processes: the example of Mont Baduel profile (French Guiana). Palaeogeogr Palaeoclimatol Palaeoecol 148(4):209

Theveniaut H, Freyssinet P (2002) Timing of lateritization on the Guiana shield: synthesis of paleomagnetic results from French Guiana and Suriname. Palaeogeography, Palaeoclimatol Palaeoecol 178(1–2): 91

Thiry M, Simon-Coinçon R, Quesnel F, Wyns R (2005) Altération bauxitique associée aux argiles à chailles Sur la bordure Sud-Est du bassin de Paris [Bauxite alteration associated with chailles clays on the south-eastern edge of the Paris basin]. Bull Soc Géol France 176(2):199–214

Twidale CR, Bourne JA (2009) On the origin of A-tents (pop-ups), sheet structures, and associated forms. Progr Phys Geogr 33(2):147−162. https://doi.org/10.1177/0309133309338660

Vasseur G, Lachassagne P (2019) Thermal disturbance caused by weathering of crystalline rocks Geological Society of London Special Publication. In: Ofterdinger U, Macdonald AM, Comte J-C, Young ME (eds) Groundwater in fractured bedrock environments. Geol Soc Lond Spec Publ 479. https://doi.org/10.1144/SP479.7

Vassolo S, Neukum C, Tiberghien C, Heckmann M, Hahne Désiré K, Baranyikwa D (2019) Hydrogeology of a weathered fractured aquifer system near Gitega, Burundi. Hydrogeol J 27:625. https://doi.org/10.1007/s10040-018-1877-0

Vidal Romani JR, Twidale CR (1999) Sheet fractures, other stress forms and some engineering implications. Geomorphology 31(1999):13–27

Vouillamoz JM, Lawson FMA, Yalo N, Descloitres M (2014) The use of magnetic resonance sounding for quantifying specific yield and transmissivity in hard rock aquifers: the example of Beni. J Appl Geophys 107(2014):16–24. https://doi.org/10.1016/j.jappgeo.2014.05.012

Vouillamoz JM, Lawson FMA, Yalo N, Descloitres M (2015) Groundwater in hard rocks of Benin: regional storage and buffer capacity in the face of change. J Hydrol 520(2015):379–386. https://doi.org/10.1016/j.jhydrol.2014.11.024

Wilford JR, Searle R, Thomas M, Pagendam D, Grundy MJ (2016) A regolith depth map of the Australian continent. Geoderma 266(2016):1–13. https://doi.org/10.1016/j.geoderma.2015.11.033

Worthington SRH, Davies GJ, Alexander EC Jr (2016) Enhancement of bedrock permeability by weathering. Earth-Sci Rev 160(2016):188–202 https://doi.org/10.1016/j.earscirev.2016.07.002

Wright EP (1992) The hydrogeology of crystalline basement aquifers in Africa. In: Wright EP, Burgess W (eds) Hydrogeology of crystalline basement aquifers in Africa. Geol Soc Lond Spec Publ 66:1–27

Wubda M, Descloitres M, Yaloc N, Ribolzi O, Vouillamoz JM, Boukari M, Hector B, Séguis L (2017) Time-lapse electrical surveys to locate infiltration zones in weathered hard rock tropical areas. J Appl Geophys 142(2017):23–37. https://doi.org/10.1016/j.jappgeo.2017.01.027

Wyns R (1991) Evolution tectonique du bâti armoricain oriental au Cénozoïque d'après l'analyse des paléosurfaces continentales et des déformations géologiques associées [Structural evolution of the Armorican basement during the Cenozoic deduced from analysis of continental paleosurfaces and associated deposits]. Géol Fr 1991(3):11–42

Wyns R (1997) Essai de quantification de la composante verticale de la déformation finie cénozoïque d'après l'analyse des paléosurfaces et des sédiments associés [Quantification test of the vertical component of the finite Cenozoic deformation based on the analysis of paleosurfaces and associated sediments]. Proceedings des Journées Scientifiques CNRS - ANDRA, Poitiers, France, 1997, pp 36–38

Wyns R (2002) Climat, eustatisme, tectonique: quels contrôles pour l'altération continentale? Exemple des séquences d'altération cénozoïques en France [Climate, eustatism, tectonics: what are the controls for continental alteration? Example of Cenozoic alteration sequences in France]. Bull Inf Géol Bass Paris 39(2):5–16

Wyns R (2012) Etude géologique du cadre structural et des forages du bassin versant de recherche du Ringelbach (Soultzeren, Haut-Rhin) [Geological study of the structural framework and of the boreholes of the Ringelbach research watershed (Soultzeren, Haut-Rhin)]. Report BRGM/RP-56540-FR, BRGM, Orléans, France, 123 pp

Wyns R (2015) Les aquifères de socle sont aussi des réservoirs pétroliers [Hardrock aquifers are also hydrocarbon reservoirs]. In: Vingtièmes journées techniques du Comité Français d'Hydrogéologie de l'Association Internationale des Hydrogéologues. « Aquifères de socle: le point sur les concepts et les applications opérationnelles » La Roche-sur-Yon, juin 2015. BRGM, Orléans, France. https://www.researchgate.net/profile/Robert-Wyns/publication/279188639_Hard_Rock_Aquifers_are_also_Hydrocarbon_Reservoirs_Poster/links/558d3e3908ae1f30aa8168b2/Hard-Rock-Aquifers-are-also-Hydrocarbon-Reservoirs-Poster.pdf. Accessed April 2021

Wyns R (2020a) Altérations supergènes et géodynamique de la lithosphère [Weathering and lithosphere geodynamics]. Géochronique 1:70–80

Wyns R (2020b) Les paléoprofils d'altération dans les Vosges et leurs applications [Weathering paleoprofiles in Vosges and their applications]. Bull Inf Géol Bass Paris 57(4):13–27

Wyns R, Clément JP, Lardeux H, Gruet M, Moguedet G, Biagi R, Ballèvre M (1998) Carte géologique de la France (1/50. 000) [Geological map of France (1/50,000)]. Sheet Chemillé no. 483. BRGM, Orléans, France

Wyns R, Gourry J-C, Baltassat J-M, Lebert F (1999) Caractérisation multiparamètres des horizons de subsurface (0-100 m) en contexte de socle altéré [Multiparameter characterization of subsurface horizons (0–100 m) in a weathered basement context]. PANGEA 31(32):51–54

Wyns R, Lacquement F, Corbier P, Vairon J (2002) Cartographie de la réserve en eau souterraine du massif granitique de la Roche sur Yon [Mapping of the underground water reserve of the granite massif of La Roche sur Yon]. Report BRGM/RP-51633/FR:26, BRGM, Orléans, France

Wyns R, Quesnel F, Simon-Coinçon R, Guillocheau F, Lacquement F (2003) Major weathering in France related to lithospheric deformation. Géol Fr 2003(1):79–87

Wyns R, Baltassat JM, Lachassagne P, Legtchenko A, Vairon J (2004) Application of proton magnetic resonance soundings to groundwater reserves mapping in weathered basement rocks (Brittany, France). Bull Soc Géol France 175(1):21–34

Wyns R, Quesnel F, Lacquement F, Bourgine B, Mathieu F, Lebert F, Baltassat JM, Bitri A, Mathon D (2005) Cartographie quantitative des propriétés du sol et du sous-sol dans la région des Pays de la Loire [Quantitative mapping of soil and subsoil properties in the Pays de la Loire region]. BRGM report RP-53676-FR, BRGM, Orléans, France, 135 pp

Wyns R, Guillou-Frottier L, Girard JP, Beauvais A, Blanc Ph (2015) Réactions exothermiques dans les profils latéritiques sur granites: conséquences sur les eaux souterraines [Exothermic reactions in lateritic profiles on granites: consequences for groundwater). In: Proceedings of Hard-Rock Aquifers: Up-to-date Concepts and Practical Applications (Aquifères de socle: le point sur les concepts et les applications opérationnelles). 20th "Technical Days" of the International Association of Hydrogeologists French Chapter, La Roche-sur-Yon, Vendée, France, June 11–13, 2015

Yao TK, Fouché O, Kouadio EK (2015) Modélisation de la surface piézométrique des aquifères fissurés en zone de socle précambrien métamorphisé: cas du bassin versant du Sassandra (sud-ouest de la Côte d'Ivoire) [Modeling of the piezometric surface of fissured aquifers in a metamorphosed Precambrian basement zone: case of the Sassandra watershed (south-west of Côte d'Ivoire)]. Rev Sci Eau 28(2):75–87

Zaidi F, Ahmed S, Dewandel B, Maréchal JC (2007) Optimizing a piezometric network in the estimation of the groundwater budget: a case study from a crystalline-rock watershed in southern India. Hydrogeol J 15(6):1131